MOLECULAR AND CELLULAR BIOLOGY, July 1999, p. 5218–5234 Vol. 19, No. 7
0270-7306/99/$04.00+0

Spatial Organization of the Core Region of Yeast TFIIIB-DNA Complexes

JIM PERSINGER, SAROJINI M. SENGUPTA, AND BLAINE BARTHOLOMEW*

Department of Biochemistry and Molecular Biology, Program of Molecular Biology, Microbiology, and Biochemistry, Southern Illinois University School of Medicine, Carbondale, Illinois 62901-4413

Received 24 July 1998/Returned for modification 1 September 1998/Accepted 29 March 1999

The interaction of yeast TFIIIB with the region upstream of the *SUP4* tRNA^{Tyr} gene was extensively probed by use of photoreactive phosphodiesters, deoxyuridines, and deoxycytidines that are site specifically incorporated into DNA. The TATA binding protein (TBP) was found to be in close proximity to the minor groove of a TATA-like DNA sequence that starts 30 nucleotides upstream of the start site of transcription. TBP was cross-linked to the phosphate backbone of DNA from bp −30 to −20 in the nontranscribed strand and from bp −28 to −24 in the transcribed strand (+1 denotes the start site of transcription). Most of the major groove of DNA in this region was shown not to be in close proximity to TBP, thus resembling the binding of TBP to the TATA box, with one notable exception. TBP was shown to interact with the major groove of DNA primarily at bp −23 and to a lesser degree at bp −25 in the transcribed strand. The stable interaction of TBP with the major groove at bp −23 was shown to require the B″ subunit of TFIIIB. The S4 helix and flanking region of TBP were shown to be proximal to the major groove of DNA by peptide mapping of the region of TBP cross-linked at bp −23. Thus, TBP in the TFIIIB-*SUP4* gene promoter region is bound in the same direction as TBP bound to the TATA box with respect to the transcription start site. The B″ and TFIIB-related factor (BRF) subunits of TFIIIB are positioned on opposite sides of the TBP-DNA core of the TFIIIB complex, as indicated by correlation of cross-linking data to the crystal structure of the TBP-TATA box complex. Evidence is given for BRF binding near the C-terminal stirrup of TBP, similar to that of TFIIB near the TBP-TATA box complex. The protein clamp formed around the TBP-DNA complex by BRF and B″ would help explain the long half-life of the TFIIIB-DNA complex and its resistance to polyanions and high salt. The path of DNA traversing the surface of TBP at the 3′ end of the TATA-like element in the *SUP4* tRNA gene is not the same as that of TBP bound to a TATA box element, as shown by the cross-linking of TBP at bp −23.

The TATA binding protein (TBP) is a subunit common to transcription factors required for promoter-dependent transcription by RNA polymerases (Pol) I (SL-1 and TIF-IB), II (TFIID), and III (TFIIIB) (19, 43, 47). Pol-specific polypeptides are associated with TBP in each of these different transcription factors and are referred to as TBP-associated factors (TAFs) (16). TBP binds to the DNA sequence TATAAAA and severely bends DNA through contacts with the minor groove of DNA (32, 33, 39). TBP forms a saddle-like structure, contacts DNA with the underside part of the saddle, and kinks the DNA at two discrete locations. TBP binds slowly to DNA, and removal of the nonconserved N-terminal portion of the protein increases the efficiency of binding to DNA (20–22, 46). In some cases, the transcription factors containing TBP are recruited to DNA through protein-protein interactions and apparently not by direct DNA-protein interactions with TBP. The *SUP4* tRNA^{Tyr} gene from *Saccharomyces cerevisiae* is an example: TFIIIB is recruited to DNA by protein-protein interactions with TFIIIC (25).

Yeast TFIIIC is a large multisubunit protein that binds to two internal promoter elements of tRNA genes, referred to as *box A* and *box B*, and helps position TFIIIB upstream of the start site of transcription (25, 27). The TFIIIB-DNA complex is resistant to polyanions and high salt. TATA-like sequences within the upstream region provide additional criteria for TFIIIB binding site preference and can alter the binding of TFIIIB within an ~20-bp region (24). TFIIIB consists of three subunits: TBP, TFIIB-related factor (BRF), and B″ (TFC5) (10, 28, 30). BRF binds directly to TFIIIC-DNA complexes (as shown by a gel shift assay) and facilitates the binding of TBP. The addition of TBP to the BRF-TFIIIC-DNA complex enhances the binding of BRF to DNA upstream of the transcription start site, as shown by DNA photoaffinity labeling (28). TBP-BRF-TFIIIC-DNA complexes are sensitive to high salt and polyanions and cannot mediate Pol III binding or transcription (1, 3). TFIIIB bends DNA to a greater degree than TBP, and the DNA is less bent in the TBP-BRF-TFIIC-DNA complex than in the complete TFIIIB-DNA complex (6, 36).

TFIIIB can also bind to DNA without TFIIIC when a TATA box is present. The yeast U6 snRNA gene contains a TATA box upstream of the start site of transcription and is transcribed in vitro with TFIIIB and Pol III (51). Although TFIIIC is not required for in vitro transcription of the U6 snRNA gene, it is required for in vivo transcription of this gene (7, 13). The in vivo role of TFIIIC in the transcription of the U6 snRNA gene is to alter a repressive chromatin structure and recruit TFIIIB (9, 15). TFIIIB does not usually bind TATA box elements in an orientation-specific manner; thus, transcription can occur in both directions from TATA box elements (51). Rather than trying to adjust the conditions either by deletion of the N-terminal nonconserved region of TBP or by inserting bulges into the DNA template so as to bias the binding of TBP and TFIIIB to DNA (11, 18), we have opted for what we think is the more relevant situation, in which TFIIIB is recruited to DNA in one unique orientation by TFIIIC. We have chosen not to investigate TFIIIB-DNA complexes that are assembled

* Corresponding author. Mailing address: Department of Biochemistry and Molecular Biology, Southern Illinois University School of Medicine, 1245 Lincoln Dr. #229C, Carbondale, IL 62901-4413. Phone: (618) 453-6437. Fax: (618) 453-6440. E-mail: bbartholomew@som.siu.edu.

independently of TFIIIC, because although they can form transcriptionally active complexes, they are likely not to be representative of in vivo complexes.

We have focused on characterizing the region upstream of the *SUP4* tRNA gene that is involved in TFIIIB binding. Three kinds of DNA photoaffinity probes were used to scan the major and minor grooves of DNA. One set of probes examined primarily the major groove of DNA (AB and DB probes), and another set of probes examined both the major and the minor grooves (S-P probes). The AB and DB probes tethered phenylazide or phenyldiazirine, respectively, to the C-5 of deoxyuridine or the N-4 of deoxycytidine. At the most extended conformation of the tether, the photoreactive site is positioned at the edge of the major groove of DNA, as shown by molecular modeling (results not shown). The DB probes were crucial in ensuring that all potential protein-DNA interactions in the major groove were determined by use of phenyldiazirine to generate the highly reactive carbene, which does not have an amino acid side-chain preference (4, 8, 38). Our cross-linking results indicate that TBP is associated with the TATA-like DNA sequence beginning 30 nucleotides upstream of the start site of transcription. TBP was shown to bind primarily to the minor groove of DNA, and this observation is consistent with the known crystal structure of the TBP-TATA box complex. Significant alteration of the TBP-DNA interface in the TFIIIB-DNA complex from that of the crystal structure of the TBP-TATA box complex was shown by site-specific DNA cross-linking and peptide mapping of photoaffinity-labeled TBP. Evidence is given for the stereospecific binding of the BRF and B″ subunits of TFIIIB to the TBP-DNA core, forming a protein clamp around DNA.

MATERIALS AND METHODS

Preparation of immobilized DNA. The nontranscribed strand of the *SUP4* $tRNA^{Tyr}$ gene containing an upstream mutant boxB was immobilized as described previously (35). The procedure for the preparation of immobilized transcribed-strand DNA was the same as that for the nontranscribed strand, except for the use of different restriction enzyme sites. pTZ1 DNA was first digested with *Eco*RI and then biotinylated by filling in the 5′ overhangs with Bio-14-dATP and Bio-11-dUTP (GIBCO BRL) by use of the Klenow fragment of DNA Pol I (U.S. Biochemicals). It was subsequently digested with *Hin*dIII and *Pvu*II, and the resulting 315- and 44-bp biotinylated fragments were bound to Dynabeads M-280–streptavidin (Dynal).

Coupling of *p*-azidophenacyl bromide to phosphorothioate-containing oligonucleotides. All procedures with photosensitive reagents were performed with indirect lighting from a 40-W incandescent lamp. Oligonucleotides containing phosphorothioates at the phosphodiester linkage between the third and fourth nucleotides from the 3′ end were resuspended in 100 mM triethylammonium bicarbonate (pH 8.0) to obtain a final concentration of 100 pmol/μl. The coupling reaction was carried out by adding 75 μl of the respective oligonucleotide to 75 μl of 100 mM *p*-azidophenacyl bromide in acetonitrile and incubating the mixture at 25°C for 4 h.

After the incubation, the solvent was evaporated from each sample by vacuum centrifugation. The pellet was resuspended in 100 μl of sterile deionized water, and the solution was extracted three times with water-saturated isobutanol and four times with water-saturated ethyl ether. The residual ethyl ether was evaporated by heating the samples at 37°C for 15 min. The modified oligonucleotides were diluted in 10 mM Tris-HCl (pH 8.0)–1 mM EDTA containing 0.05% Tween 20 to a final concentration of 2 pmol/μl. The extent of modification was determined by enzymatically incorporating a single α-^{32}P-deoxynucleotide at the 3′ end by primer extension and analyzing the products of modified versus unmodified oligonucleotides on a denaturing 10% polyacrylamide gel. The extent of modification ranged from 45 to 80%.

Synthesis of DNA photoaffinity probes. Double-stranded DNA probes containing modified phosphodiesters were prepared by annealing modified oligonucleotides to an immobilized single-stranded DNA template with heating at 70°C for 3 min, followed by cooling at 37°C for 30 min in buffer A (30 mM Tris-HCl [pH 8.0], 50 mM KCl, 7 mM $MgCl_2$, 0.05% Tween 20). Reducing agents such as dithiothreitol were avoided so as not to reduce the phenylazido moiety (41). The beads were washed three times with buffer A containing 0.1 mg of bovine serum albumin per ml. An α-^{32}P-deoxynucleotide (specific activity, 2,000 to 3,000 Ci/mmol) was enzymatically incorporated with the Klenow fragment of DNA Pol I, and probe synthesis was continued as described above to make DNA double stranded over the entire stretch of the DNA probe (35).

5-[*N*-(4-Azidobenzoyl)-3-aminoallyl]-dUTP (AB-dUTP), 4-[*N*-(4-azidobenzoyl)-2-aminoethyl]-dCTP (AB-dCTP), and 5-{*N*-[4-[3-(trifluoromethyl)-diazirin-3-yl]benzoyl]-3-aminoallyl}-dUTP (DB-dUTP) were synthesized as described previously (2, 35, 49). 4-{*N*-[*p*-[3-(Trifluoromethyl)-diazirin-3-yl]benzoyl]-2-aminoethyl}-dCTP (DB-dCTP) was prepared by adding 50 μl of 100 mM 4-[3-(trifluoromethyl)-diazirin-3-yl]benzoate *N*-hydroxysuccinimide to 50 μl of 13 mM N^4-(aminoethyl)-dCTP in 100 mM sodium borate (pH 8.5). The mixture was incubated at 25°C for 4 h. DB-dCTP was purified by ion-exchange chromatography with DEAE–A-25 Sephadex and analyzed by thin-layer chromatography as described previously (35).

DNA probes containing 5-[*N*-(4-azidobenzoyl)-3-aminoallyl]-dUMP (AB-dUMP) and 5-{*N*-[4-[3-trifluoromethyl]-diazirin-3-yl] benzoyl-3-aminoethyl}-dUMP (DB-dUMP) at positions −27, −20, −16, and −11 on the transcribed strand and at positions −30, −26, −24, −22/−21, −17, and −12 on the nontranscribed strand were prepared as described previously (41). Photoreactive probes containing 4-[*N*-(4-azidobenzoyl)-2-aminoethyl]-dCMP (AB-dCMP) at nucleotide positions −25, −23, and −18 and 4-{*N*-[4-trifluoromethyl]-diazirin-3-yl] benzoyl-3-aminoallyl}-dCMP (DB-dCMP) at nucleotide position −23 on the transcribed strand were synthesized in the same manner as the other probes.

For all the above-mentioned positions, with the exception of the −20 and −19 probes, the photoreactive nucleotide was incorporated first. The immobilized DNA was washed with buffer A containing 1 mM 2-mercaptoethanol, following which a radiolabeled nucleotide was incorporated. For the −20 and −19 probes, first a nonphotoreactive, nonradiolabeled nucleotide was incorporated; then, the radiolabeled nucleotide and the photoreactive nucleotide were incorporated into DNA.

Photoaffinity labeling of the transcription complex. Transcription complexes were formed on probe DNA by use of the 500 mM KCl fraction from BioRex 70 chromatography of the S-100 extract of *S. cerevisiae* BJ926 (BR500) (35). Alternatively, transcription complexes were assembled by use of recombinant TFIIIB (rTFIIIB) and partially purified TFIIIC as described previously (30). TFIIIC was obtained from the flowthrough fractions of Ni-nitrilotriacetic acid chromatography of His-tagged RNA Pol III as described previously (35).

Photoaffinity labeling with rTFIIIB and TFIIIC was carried out in the presence and absence of B″ (apparent molecular mass, 90 kDa). The amount of protein used for efficient complex formation was determined by titrating the amount of each protein added and analyzing by gel shift analysis (27). These titrations were done by use of an amount of TBP slightly higher than needed, titrating in different amounts of BRF, and assaying for the production of TBP-BRF-TFIIIC-DNA complexes. After optimization of BRF, the amount of B″ was titrated to optimize for the production of TFIIIB-TFIIIC-DNA complex formation. Complexes formed on DNA probes containing phosphorothioates and AB nucleotides were irradiated differently from those containing DB nucleotides. For the former, microcentrifuge tubes containing the reaction mixture were placed with their caps open at a distance of 20 cm from a short-wavelength (~254-nm) UV lamp. The samples were irradiated for 2 min. DB probes were irradiated for 15 min at a distance of 7 cm from a Fotodyne transilluminator (model 3-4400). A Pyrex glass dish was placed between the samples and the transilluminator to filter out wavelengths shorter than 300 nm. Photoaffinity-labeled TBP was immunoprecipitated with anti-TBP antibody as described previously (41).

Cyanogen bromide cleavage of photoaffinity-labeled TBP and preparation of a radiolabeled TBP molecular weight standard. A large photoaffinity labeling reaction mixture (200 μl) was assembled by use of the BR500 fraction that had been treated with heparin at a final concentration of 0.15 mg/ml and placed in a multichannel pipeter basin for irradiation. The conditions for the irradiation and digestion of DNA with DNase I and S1 nuclease were the same as before (35). The protein was concentrated by ultrafiltration (Centricon 10; Millipore). Before the sample was loaded for sodium dodecyl sulfate (SDS)-polyacrylamide gel electrophoresis (PAGE), the following were added to the indicated final concentrations: 10% SDS, 0.7 M β-mercaptoethanol (BME), 0.44% bromophenol blue, 0.3 M Tris-HCl (pH 6.8), and 16% glycerol. The sample was loaded on an SDS–12% polyacrylamide gel (18 cm by 18 cm by 0.8 mm). After electrophoresis, cross-linked TBP was visualized by autoradiography, and the corresponding gel slice was excised. TBP was electroeluted from the gel slice (Bio-Rad model 422 Electro-Eluter) at 10 mA for 4 h into a volatile buffer consisting of 50 mM ammonium bicarbonate and 0.1% SDS. The eluate obtained was dried by vacuum centrifugation, resuspended in 200 μl of sterile deionized water, and dried again.

The DNA tag left attached to the protein was digested by treatment with 70% formic acid–1.4% diphenylamine at 70°C for 20 min. The sample was extracted five times with an equal volume of water-saturated ethyl ether. It was evaporated to dryness by vacuum centrifugation, resuspended in sterile deionized water, and dried again. The pellet was resuspended in 80 μl of 2% SDS–0.1 mM BME.

Cyanogen bromide cleavage was carried out by adding 1 μl of 1 M hydrochloric acid and 1 μl of 1 M cyanogen bromide in acetonitrile to the sample, so that the final concentration of each was approximately 100 mM. The sample was incubated in the dark at 23 to 25°C for 10 min or 2 h. The sample was resolved on a 16.5% Tricine–SDS gel (44). After electrophoresis, the gel was stained with Coomassie blue G250 to visualize the low-molecular-weight standard (Pharma-

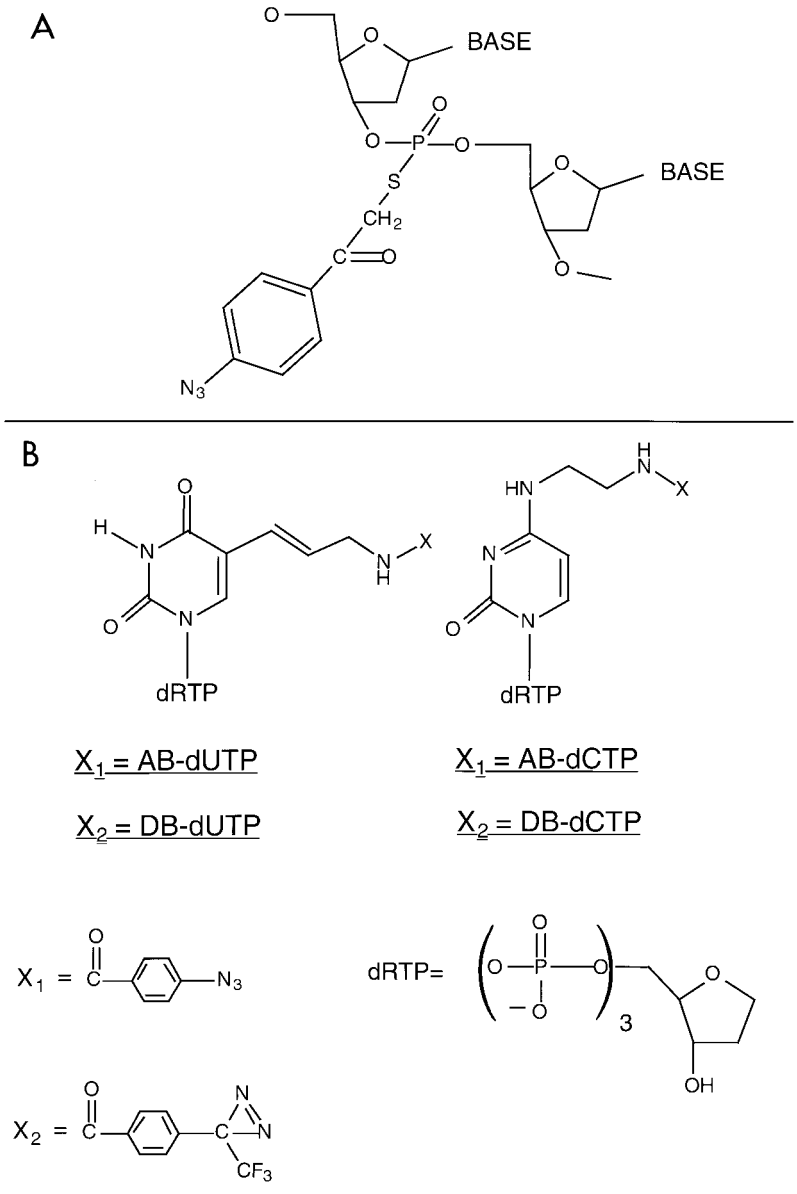

FIG. 1. Synthesis of photoreactive DNAs for probing the major and minor grooves of DNA. (A) Modification of the phosphate backbone of DNA. A phosphorothioate incorporated at a unique site in DNA is alkylated with *p*-azidophenacyl bromide to covalently couple phenylazide to the phosphate backbone. The structure of the chemical modification in DNA shown will position phenylazide in the major and minor grooves of DNA. (B) Phenylazide and phenyldiazirine are tethered to dUTP and dCTP. Phenylazido (X1) and phenyldiazirinyl (X2) groups are positioned in the major groove of DNA by covalent attachment to the C-5 of deoxyuridine or the N-4 of deoxycytidine, respectively. The tether for the attachment of the phenylazido and phenyldiazirinyl groups to the nucleotide base is the same. (C) The positions in the *SUP4* tRNA gene containing the photoreactive moiety are shown for the nontranscribed strand (top) and the transcribed strand (bottom). The modified sites are indicated in bold letters: the modified phosphodiester of the S-P probes is positioned between the two nucleotides shown in bold lowercase letters, whereas the modified nucleotide is that shown in bold for the AB and DB probes. The position of the radioactive label is underlined and is located 3 nucleotides away from the modification site for the S-P probes and is immediately adjacent to the modified nucleotide for the AB and DB probes.

cia), dried, autoradiographed, and quantitated with a Molecular Dynamics PhosphorImager.

A ladder of radiolabeled TBP fragments to be used as a molecular weight standard was prepared as follows. A phosphorylation site (GRRLSL) was engineered into wild-type TBP by changing the cysteine at amino acid 78 to an arginine and the aspartate at amino acid 81 to a serine by site-directed mutagenesis. The phosphorylation reaction mixture contained 500 pmol of mutant TBP, 300 U of heart muscle kinase (catalytic subunit; Sigma), and 375 pmol of [γ-^{35}S]adenosine-$\gamma\alpha$-thiotriphosphate (~2,000 Ci/mmol) in a final volume of 150 μl of buffer B (20 mM Tris-HCl [pH 7.6], 100 mM NaCl, 12 mM $MgCl_2$, 0.2 mM EDTA, 0.5 mg of bovine serum albumin per ml, 0.05% Tween 20) and was incubated for 1 h at 30°C. Unincorporated ^{35}S-ATP was removed from the sample by ultrafiltration (Centricon 10). Phosphorylated TBP was gel purified and cleaved with cyanogen bromide as described earlier for photoaffinity-labeled TBP. Wild-type TBP was not detectably phosphorylated under identical conditions.

In order to allow for more complete cleavage of photoaffinity-labeled TBP, the following procedure was carried out. A 300-μl reaction mixture consisting of the BR500 fraction and the AB-dCMP DNA probe at bp −23 was assembled. After irradiation, the DNA was cleaved with 70% formic acid–1.4% diphenylamine for 20 min at 70°C. The sample was extracted and dried as described earlier. The pellet was resuspended in sterile deionized water and precipitated with acetone. The precipitated protein was resuspended in sample loading buffer (10% SDS, 0.7 M BME, 0.44% bromophenol blue, 0.3 M Tris-HCl [pH 6.8], 16% glycerol) and loaded on an SDS–4 to 20% polyacrylamide gel.

After electrophoresis, the protein was electroblotted onto a polyvinylidene difluoride (PVDF) membrane. Photoaffinity-labeled TBP was visualized by auto-

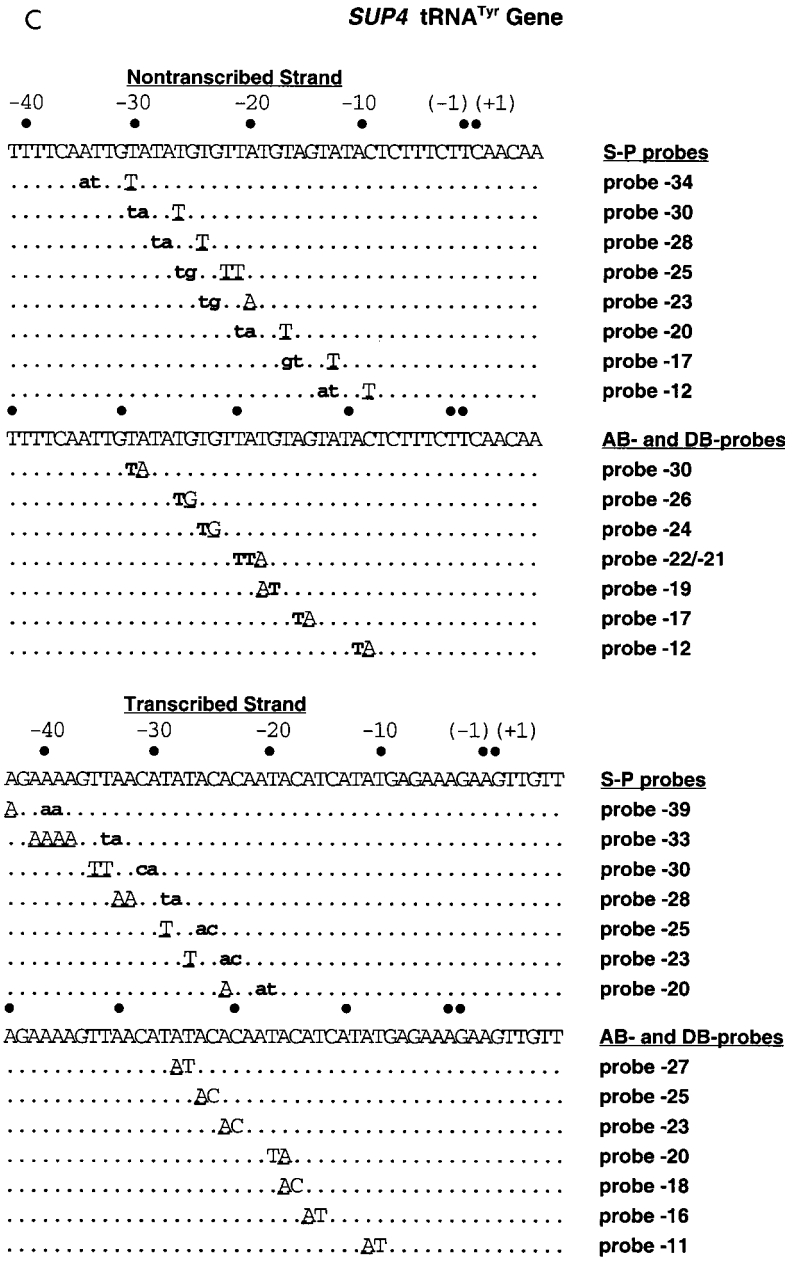

FIG. 1—*Continued.*

radiography, and the corresponding band was excised. The membrane slice was cut into smaller pieces and washed with 500 μl of cold 95% acetone. The acetone was discarded, and 150 μl of 150 mM cyanogen bromide in 70% formic acid was added to the membrane pieces. The sample was incubated in the dark at room temperature for 24 h with continuous, gentle vortexing. The supernatant was transferred and dried by vacuum centrifugation. One hundred microliters of 40% acetonitrile was added to the PVDF pieces, the sample was incubated at 37°C for 3 h, and the supernatant was removed. One hundred microliters of 0.05% trichloroacetic acid–40% acetonitrile was added to the membrane pieces, and the sample was heated for 20 min at 50°C. The supernatants were combined, and the solvent was removed by vacuum centrifugation. The pellet was resuspended in 60 μl of sterile water and dried a second time. The pellet was then resuspended in buffer C (24% glycerol, 0.2 M Tris-HCl [pH 6.8], 1.1 M 2-mercaptoethanol, 12% SDS, 0.08% Coomassie blue G250) and loaded on a 16.5% Tricine–SDS gel.

Cleavage of photoaffinity-labeled TBP with 2-nitro-5-thiocyanobenzoic acid (NTCB). A large-scale photoaffinity labeling reaction with TFIIIB, six-His-tagged TBP, and partially purified TFIIIC was set up. The cross-linked sample was concentrated approximately 20-fold by ultrafiltration (Centricon 10). The DNA was digested with formic acid-diphenylamine, extracted, and dried as described above for the cleavage with cyanogen bromide. The pellet was resuspended in sample loading buffer, and photoaffinity-labeled TBP was purified by SDS-PAGE as described earlier. The eluted protein was diluted to 2 ml with 8 M urea–0.2 M Tris acetate (pH 8) and concentrated by ultrafiltration (Centricon 10). The sample was diluted and concentrated two more times with the same solution.

TBP was reduced by treatment with 10 mM 2-mercaptoethanol for 30 min at 37°C. The free sulfhydryl groups were modified with 10 mM NTCB at 37°C for 30 min (23). The pH of the sample was adjusted to 9.0 with 5 M NaOH. Cleavage at the modified cysteines was allowed to occur at 37°C for 6 h, after which the pH was readjusted to pH 8 with acetic acid. Buffer C was added to samples taken out of the reaction mixture at different stages and analyzed on a 16.5% Tricine–SDS gel, stained with Coomassie blue G250, and autoradiographed as described earlier.

RESULTS

We have examined the protein-DNA contacts of a TFIIIC-dependent TFIIIB-DNA complex to determine the functional and structural features of TBP in a complex where TBP is not

the exclusive determinant of the DNA binding specificity. A region spanning ~24 nucleotides (bp −11 to −34) was probed by DNA photoaffinity labeling. Two kinds of DNA photoaffinity probes were constructed to examine protein contacts exclusively in the major groove of DNA (AB and DB probes) or contacts in either the minor or the major groove of DNA (S-P probes). Photoreactive moieties were attached to the phosphate backbone of DNA with a 7-Å tether and the photoreactive moiety directed toward the major and minor grooves of DNA (S-P probes; Fig. 1A). The photoreactive group was attached to DNA by alkylation of a uniquely incorporated phosphorothioate in DNA. Eight and seven positions in the nontranscribed and transcribed strands, respectively, were modified (Fig. 1C). The radioactive label was incorporated 3 nucleotides from the modification site in the 3′ direction.

Pol III transcription complexes were formed on these modified DNA probes by use of the 500 mM eluate from BioRex 70 chromatography, which contains Pol III, TFIIIB, and TFIIIC. Pol III and TFIIIC were released from DNA by the addition of heparin (100 to 150 μg/ml), and the remaining TFIIIB-DNA complexes were cross-linked by UV irradiation. After enzymatic degradation of the DNA probes, cross-linked proteins were analyzed by SDS-PAGE and autoradiography. TBP (molecular mass, ~27 kDa) was cross-linked to DNA on the 3′ side of bp −30, −28, −25, −23, and −20 on the transcribed strand and to DNA on the 3′ side of bp −28, −26, and −24 on the nontranscribed strand (Fig. 2A, lanes 3, 5, 7, 9, and 11, and Fig. 2B, lanes 7, 9, and 15). Positions farther upstream, at bp −33 (transcribed strand) and bp −34 and −30 (nontranscribed strand), and downstream, at bp −21, −18, and −13 (nontranscribed strand), did not significantly cross-link TBP. These results are consistent with TBP binding to the TATA-like sequence, TATATGT, 30 bp upstream of the start site of transcription (Fig. 2C). TBP cross-linking was shown to require efficient binding of TFIIIC by competition with specific versus nonspecific DNAs. Equivalent amounts of carrier DNA with or without the *SUP4* tRNA gene were added to all samples. When the competitor DNA contained the *SUP4* tRNA gene, cross-linking of TBP was eliminated on both strands of DNA (Fig. 2A, lanes 4, 6, 8, 10, and 12, and Fig. 2B, lanes 8, 10, and 16).

The BRF (molecular mass, ~67 kDa) subunit was also cross-linked in a TFIIIC-dependent manner at sites within the TATA-like sequence and downstream of this region. BRF was cross-linked on the 3′ side of bp −30, −28, and −20 of the transcribed strand and on the 3′ side of bp −30, −28, −21, −18, and −13 of the nontranscribed strand (Fig. 2A, lanes 3, 5, and 11, and Fig. 2B, lanes 1, 3, 5, 13, and 15). At sites upstream of the TATA-like sequence, the B″ (molecular mass, ~90 kDa) subunit of TFIIIB was efficiently cross-linked at bp −34 and −33 of the nontranscribed and transcribed strands, respectively (Fig. 2A, lane 1, and Fig. 2B, lane 11). Interestingly, B″ was also efficiently cross-linked near the center of the TATA-like sequence to the transcribed strand at bp −25 and −23 but not to the nontranscribed strand (compare Fig. 2A, lanes 7 and 9, to Fig. 2B, lanes 7 and 9). Cross-linking on the 3′ side of bp −26 and −24 of the nontranscribed strand showed a lack of efficient cross-linking of either of the two largest subunits of TFIIIB (Fig. 2B, lanes 7 and 9).

The S-P (modified-phosphate-backbone) DNAs probed protein-DNA interactions in either the major or the minor groove. In order to distinguish major-groove interactions from minor-groove interactions, we used AB-dCMP and AB-dUMP to place a phenylazido group into the major groove of DNA (Fig. 1B); we compared the results obtained with these probes to those obtained with the S-P probes. The incorporation of modified nucleotides into DNA did not interfere with the formation of transcription complexes or initiation at the normal start site of transcription, as determined by multiple-round transcription assays (data not shown). TBP binds to TATA box DNA through the minor groove of DNA and directs the major groove of DNA in toward itself to create a pocket or core of DNA (32, 33). If TBP is bound to DNA in the TFIIIB-DNA complex as it is to the TATA box, then TBP would not be expected to be cross-linked with the AB probes. Of the 14 different sites in DNA scanned in the nontranscribed and transcribed strands, 12 positions showed no significant amount of photoaffinity labeling of TBP (Fig. 3A and B). TBP was, however, cross-linked to DNA at a very discrete region in the transcribed strand at bp −23 and fivefold less at bp −25 in the preinitiation complex (Fig. 3A, lanes 9 and 10). Cross-linking of TBP, BRF, and B″ at these positions was shown by DNA competition to be promoter specific and to require the efficient binding of TFIIIC (results not shown). All the reactions shown in Fig. 3 contained, on a molar basis, 200 times more linearized plasmid DNA (pLNG56) containing one copy of a defective *SUP4* tRNA gene than did the photoreactive DNA probe. The *SUP4* tRNA gene in pLNG56 has two point mutations in the *box B* element and binds TFIIIC 300 times less efficiently than does the DNA probe. Cross-linking of TBP, BRF, and B″ was eliminated when plasmid DNA (pTZ1) containing the same version of the *SUP4* tRNA gene as the DNA photoaffinity probe was substituted for pLNG56 DNA.

Specific cross-linking of the 34-kDa subunit of Pol III was observed at bp −17 and −16 (Fig. 3A, lanes 6 and 13), and that of the 160-kDa subunit was observed at bp −11 and −12 (lanes 7 and 14), consistent with previous reports (1, 35). Proteins cross-linked at bp −27 were not promoter specific, and the low amount of cross-linking of the ~30- to 50-kDa proteins at bp −22 and −21 was also not specific (results not shown). The 128-kDa subunit of Pol III and the 120-kDa subunit of TFIIIC were most intensely cross-linked at bp −22 and −21 and at bp −17 and −12 (Fig. 3A, lanes 4, 6, and 7). The ~170-kDa protein labeled at bp −22 and −21 appears not to be part of the Pol III transcription complex and is cross-linked independently of TFIIIC. An ~50-kDa protein is labeled at bp −17 and −16 in a promoter-dependent manner (Fig. 3A, lanes 6 and 13, and results not shown).

Pol III and TFIIIC were removed from DNA by the addition of heparin to examine the contacts of TFIIIB alone bound to DNA (31). Cross-linking of TBP was still observed only at bp −23 and −25 on the transcribed strand and with the same efficiency as in the preinitiation complex (Fig. 3B, compare lanes 9 and 10 to lanes 15 and 16). Labeling of the BRF and B″ subunits was also heparin resistant and was enhanced at some positions, presumably due to the removal of TFIIIC and Pol III. The photoaffinity-labeled ~27-kDa protein was confirmed to be TBP by immunoprecipitation with anti-TBP antibody (Fig. 3C, lanes 1 and 6).

The influence of B″ on TBP interactions with the major groove was analyzed by performing photoaffinity labeling experiments with TFIIIB reconstituted by use of recombinant BRF, TBP, and B″. In the presence of B″, TBP was cross-linked on the transcribed strand at bp −23 and, to a minor extent, at bp −25 and −18 (Fig. 4A, lanes 3, 5, and 9). In the absence of B″, TBP was cross-linked nine times less efficiently on the transcribed strand at bp −23 (Fig. 4A, compare lanes 5 and 6). In the absence of B″, TBP was labeled on the nontranscribed strand at bp −33 and −32 and much less intensely at bp −30 and at bp −22 and −21 (Fig. 4B, lanes 4, 6, and 10). Photoaffinity labeling of TBP in the absence of B″ is dependent on the prior interaction of TFIIIC and BRF with DNA, as shown by DNA competition experiments with pTZ1 DNA versus

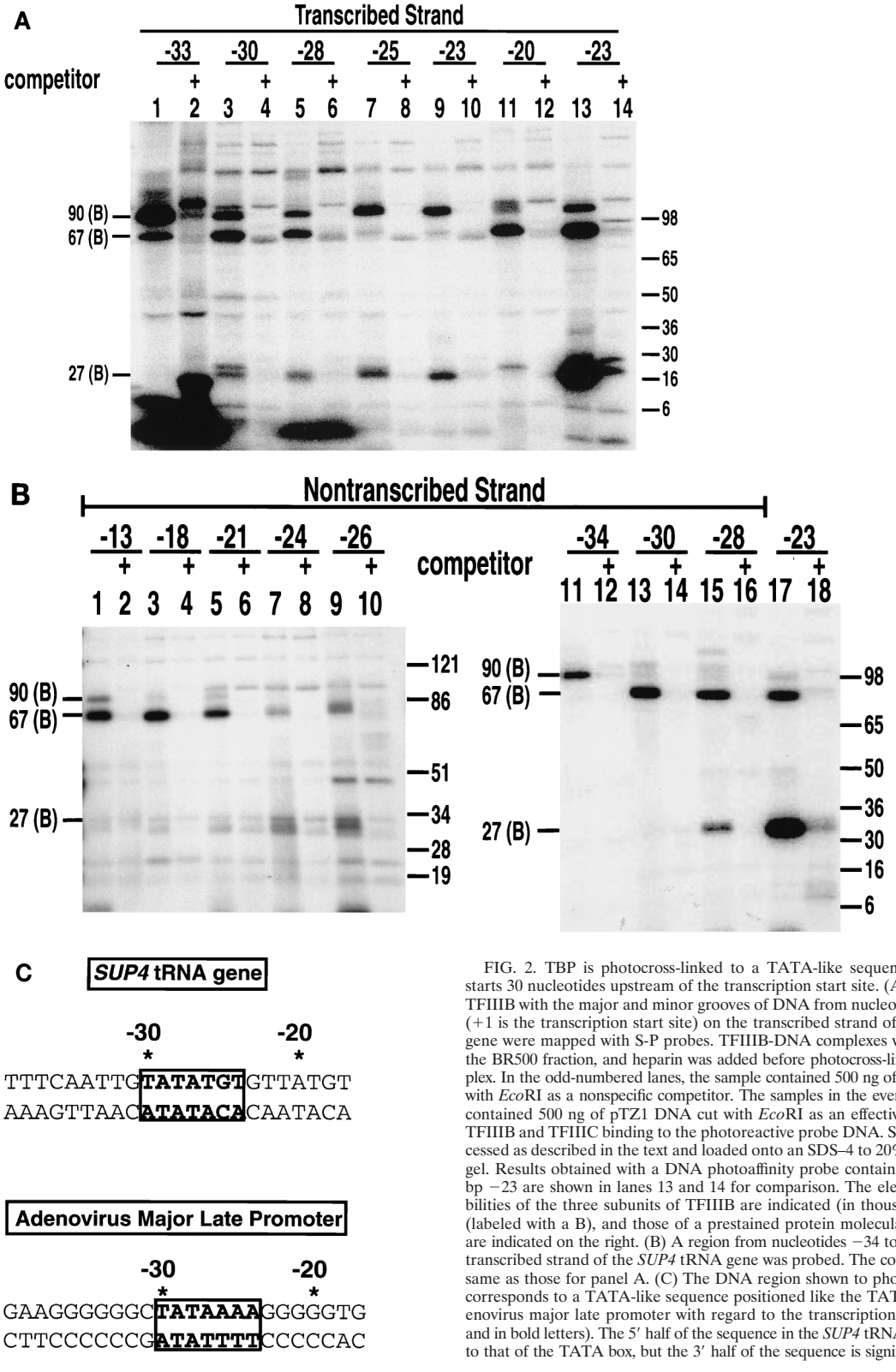

FIG. 2. TBP is photocross-linked to a TATA-like sequence of DNA that starts 30 nucleotides upstream of the transcription start site. (A) Interactions of TFIIIB with the major and minor grooves of DNA from nucleotides −33 to −20 (+1 is the transcription start site) on the transcribed strand of the *SUP4* tRNA gene were mapped with S-P probes. TFIIIB-DNA complexes were formed with the BR500 fraction, and heparin was added before photocross-linking of the complex. In the odd-numbered lanes, the sample contained 500 ng of pGEM DNA cut with *Eco*RI as a nonspecific competitor. The samples in the even-numbered lanes contained 500 ng of pTZ1 DNA cut with *Eco*RI as an effective competitor for TFIIIB and TFIIIC binding to the photoreactive probe DNA. Samples were processed as described in the text and loaded onto an SDS–4 to 20% polyacrylamide gel. Results obtained with a DNA photoaffinity probe containing AB-dCMP at bp −23 are shown in lanes 13 and 14 for comparison. The electrophoretic mobilities of the three subunits of TFIIIB are indicated (in thousands) on the left (labeled with a B), and those of a prestained protein molecular weight marker are indicated on the right. (B) A region from nucleotides −34 to −13 on the nontranscribed strand of the *SUP4* tRNA gene was probed. The conditions were the same as those for panel A. (C) The DNA region shown to photocross-link TBP corresponds to a TATA-like sequence positioned like the TATA box of the adenovirus major late promoter with regard to the transcription start site (boxed and in bold letters). The 5′ half of the sequence in the *SUP4* tRNA gene is identical to that of the TATA box, but the 3′ half of the sequence is significantly different.

pLNG56 DNA (data not shown). The addition of B″ enhanced the cross-linking of TBP to DNA at bp −23 and eliminated TBP cross-linking at bp −33 and −32, at bp −30, and at bp −22 and −21 on the nontranscribed strand. As previously noted, B″ also enhanced the cross-linking of BRF at bp −38 to −23, while in this same region, the cross-linking of the 120-kDa subunit of TFIIIC was greatly diminished because of direct or indirect displacement or competition by B″ (Fig. 4A,

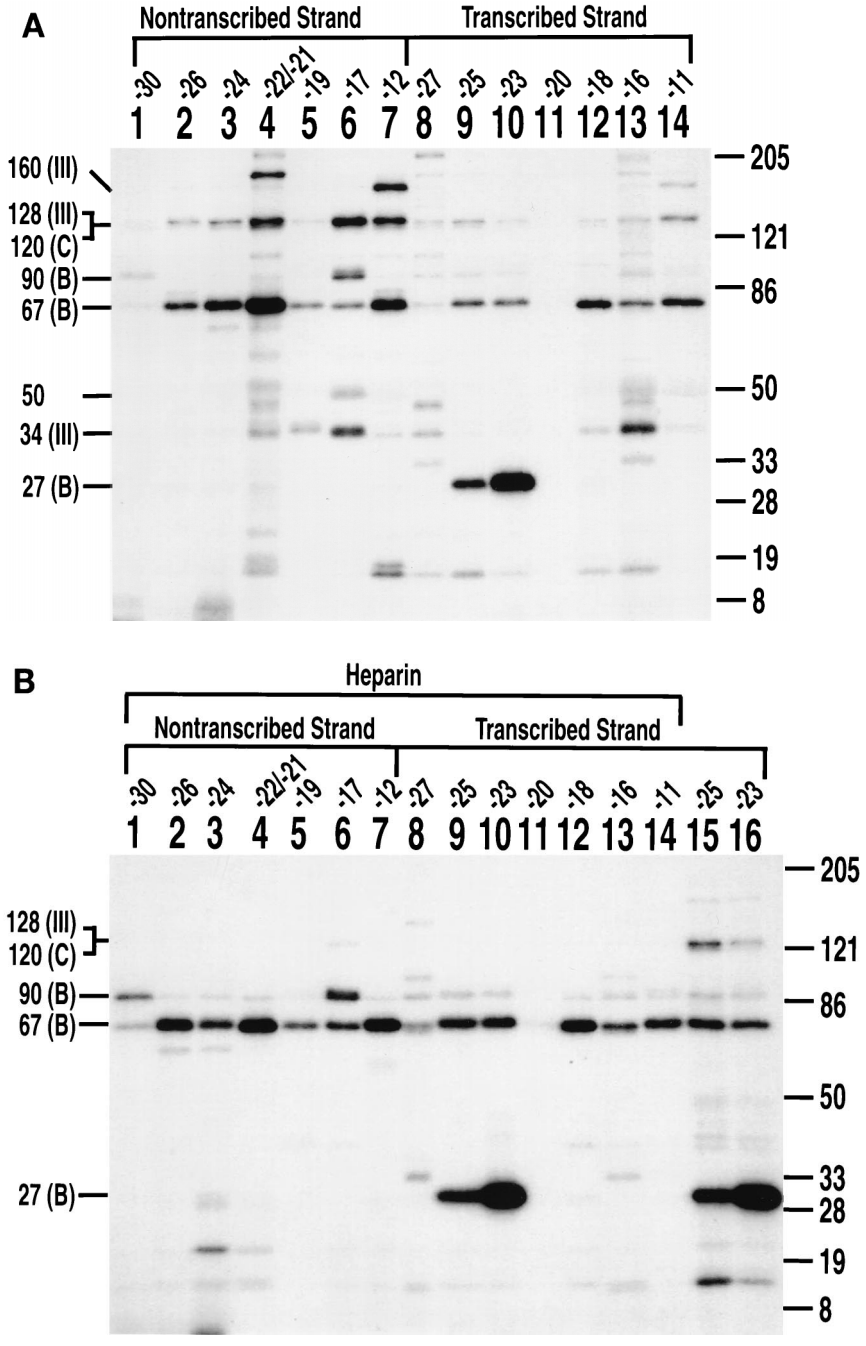

FIG. 3. TBP is photocross-linked primarily through the minor groove, except at bp −23 and −25 on the transcribed strand. (A) Photocross-linking experiments with the preinitiation complex were carried out with 14 probes containing AB-dUMP (lanes 1 to 8, 11, 13, and 14) or AB-dCMP (lanes 9, 10, and 12) at the nucleotide positions indicated in the *SUP4* tRNA gene and analyzed by electrophoresis on an SDS–4 to 20% polyacrylamide gel. (B) Complexes were formed as in panel A, but heparin (100 μg/ml) was added to remove TFIIIC and Pol III from DNA before photocross-linking (lanes 1 to 14). Lanes 15 and 16 did not contain heparin and are similar to lanes 9 and 10 in panel A. Molecular weight markers in panels A and B are as described in the legend to Fig. 2. (C) TFIIIB-DNA complexes were photocross-linked at bp −23 in the presence of heparin, and TBP was immunoprecipitated with an anti-TBP antibody. The antigen-antibody complex was precipitated with protein A-Sepharose and analyzed by electrophoresis on an SDS–4 to 20% polyacrylamide gel. Lane 1 contains a sample before the addition of antibody to show that BRF and TBP are cross-linked [67 (B) and 27 (B), respectively]. TBP, and not BRF, was immunoprecipitated, as can be seen in a longer exposure (compare lanes 2 and 6 and results not shown). The electrophoretic mobilities of the 120-kDa subunit of TFIIIC (C); the 160-, 128-, and 34-kDa subunits of Pol III (III); and the three subunits of TFIIIB (B) are indicated on the left.

lanes 1 to 6, and Fig. 4B, lanes 1 to 8) (3, 26). These data indicate that B″ promotes the interaction of TBP with the major groove of DNA at bp −23 on the transcribed strand, whereas the cross-linking of TBP is eliminated at other positions.

In order to ensure that all the interactions of TFIIIB with the major groove of DNA were detected, DNA probes containing phenyldiazirine were constructed. Upon photolysis, phenyldiazirine produces highly reactive carbene, which does not have a preference for nucleophilic side chains, as does dehydroazepine formed by the rearrangement of phenylni-

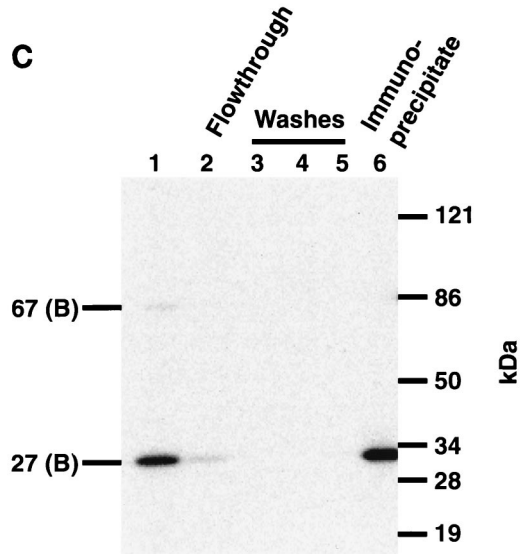

FIG. 3—*Continued.*

trene (4, 8, 14). The photoreactive nucleotides DB-dUMP and DB-dCMP have the same tether as AB-dUMP and AB-dCMP, so that photocross-linking results can be directly compared (Fig. 1B). Cross-linking of the preinitiation complexes revealed some significant differences between the phenyldiazirine- and phenylazide-containing nucleotide analogs (compare Fig. 5A and B to Fig. 3A).

The DB probes showed that the B″ subunit interacts with the major groove at bp −27 and −23 on the transcribed strand and at bp −30 on the nontranscribed strand (Fig. 5A, lanes 1 and 5, and Fig. 5B, lane 1). The AB probes inefficiently photoaffinity labeled the transcription complex at bp −30 (transcribed strand) and at bp −27 and −20 (transcribed strand) (Fig. 3A, lanes 1, 8, and 11). Although no proteins were cross-linked at bp −20 by AB-dUMP, the BRF subunit was efficiently cross-linked at this same position by DB-dUMP (compare Fig. 3A, lane 11, to Fig. 5A, lane 2). The difference between DB-dCMP and AB-dCMP cross-linking at bp −23 on the transcribed strand suggests that the efficient cross-linking of TBP by AB-dCMP is due to the proximity of a nucleophilic side chain(s) in TBP. The less efficient cross-linking of TBP by DB-dCMP at bp −23 presumably occurs because DB-dCMP does not have a side-chain preference and the B″ subunit is more prevalent (Fig. 5A, compare lanes 5 and 6). TBP was cross-linked at bp −23 on the transcribed strand and, to a minor extent, at bp −24 and at bp −22 and −21 on the nontranscribed strand. Less efficient cross-linking of the B″ subunit was also seen at bp −24 and −17 on the transcribed strand (Fig. 5B, lanes 3 and 6).

The largest subunit (160 kDa) of Pol III was cross-linked at bp −11 (transcribed strand) and at bp −12 (nontranscribed strand) with the DB probes, consistent with the cross-linking results obtained with the AB probes (Fig. 5A, lane 4, and Fig. 5B, lane 7). The 34-kDa subunit was cross-linked at bp −16 (transcribed strand) but not at bp −17 (nontranscribed strand) with the DB probes. Efficient cross-linking of an ~50-kDa protein at bp −11 was observed with DB-dUMP but not with AB-dUMP. Photoaffinity labeling of the ~50-kDa protein was TFIIIC dependent and was not changed upon the formation of a stalled elongation complex with the addition of ATP, CTP, and UTP (results not shown). Cross-linking of a similar ~50-kDa protein with AB-dUMP was previously noted at bp −9 and −8 on the nontranscribed strand (35).

A summary of where DNA cross-links to the BRF, B″, and TBP subunits of TFIIIB is shown in Fig. 6A. BRF was extensively cross-linked to the nontranscribed strand in the same region in which TBP interacts with DNA, whereas B″ was cross-linked most efficiently to the transcribed strand in this same region. TBP was cross-linked mostly in the minor-groove region, except near bp −23 on the transcribed strand. If there is significant structural similarity between the TFIIIB-DNA complex and the TBP-TATA box complex, a more comprehensive interpretation of the data can be made by correlating the cross-linking information to the known crystal structure of TBP bound to a TATA box.

Several lines of evidence from results presented here and from work by others (11, 24, 45) indicate that TBP binds to the TATA-like sequence of the tRNA gene in a manner similar to that of the TATA element found in many mRNA genes. Photoaffinity labeling with the S-P probes demonstrates that TBP is positioned at the TATA-like sequence upstream of the start site of transcription. The lack of TBP cross-linking with the AB and DB probes except around bp −23 indicates that throughout most of this region, TBP binds through the minor groove of DNA, consistent with the crystal structure. The cross-linking data from the phosphate backbone and the major groove of the *SUP4* tRNA gene were correlated to the known crystal structure of TBP bound to the TATA box of the major late promoter of adenovirus through alignment of the TATA sequence (Fig. 3C and Fig. 6B to D). Corresponding positions in the phosphate backbone and the major groove were highlighted to indicate where BRF (green) and B″ (blue) were shown to cross-link DNA.

Correlation of DNA cross-linking data to the crystal structure indicates that BRF most likely interacts with one side of the TBP-TATA box complex (Fig. 6B). The large distortion of the DNA structure due to bending by TBP causes the nontranscribed strand of the TATA box to be located on one side of TBP, whereas the transcribed strand of the TATA box is found on the opposite side of TBP. Examination of the other side of the TBP-TATA box structure shows that the B″ subunit most likely interacts extensively with this surface, thus positioning B″ on one side of TBP and BRF on the opposite side to clamp TBP in on the surface of the DNA (Fig. 6C). This kind of protein clamp could help explain the exceptionally tight DNA binding of the fully assembled TFIIIB complex. B″ appears to extend far into the hole created through positioning of the major groove inward and can be cross-linked deep into this region (Fig. 6C, −30 NTS, −27 TS, and −23 TS). In comparison, BRF appears to extend less into this core region created by the major groove of DNA. On the surface contacted primarily by B″, it is significant that the S-P probes cross-link both BRF and B″ on the 3′ side of bp −30 and −28. The S-P probes consist of two stereoisomers such that the photoreactive group is positioned in the major or minor groove. Consistent with the other positions that were scanned, B″ is probably cross-linked by the stereoisomers positioned in the major groove, and BRF is probably cross-linked by those positioned in the minor groove. This interpretation is supported by the observation that only B″ is cross-linked in the major groove at bp −27 (transcribed strand) with DB-dUMP. An interaction of BRF near the minor groove of DNA in this region on the transcribed and nontranscribed strands would be consistent with a segment of the BRF subunit contacting one stirrup of TBP, as for TFIIB and TBP (Fig. 6D).

One inconsistency between the cross-linking data and the TBP-TATA box crystal structure is that of TBP cross-linking to the major groove of DNA at bp −23. In order to better understand the structural significance of these cross-linking data

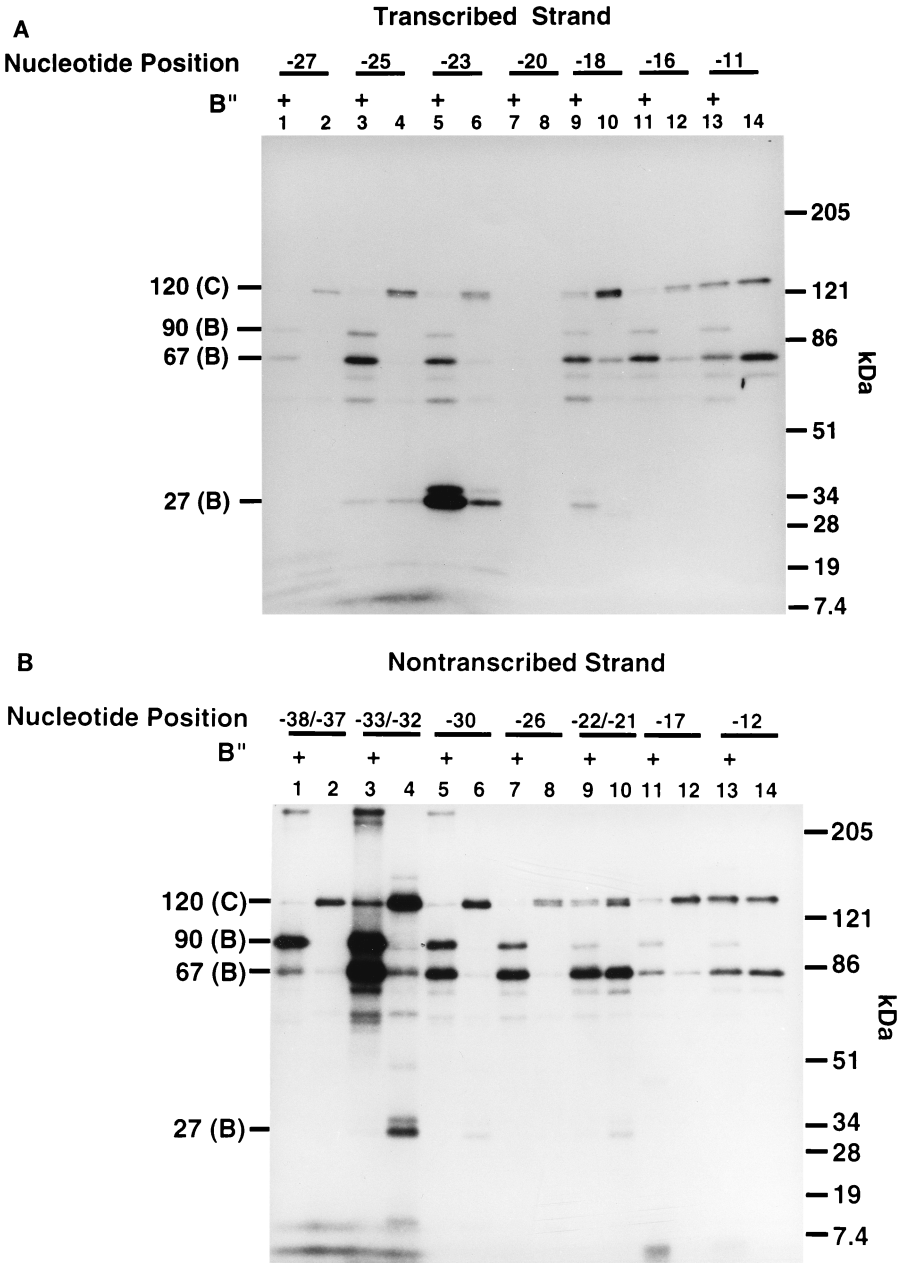

FIG. 4. B″ helps position TBP in the major groove of DNA at bp −23 on the transcribed strand. Fourteen probes containing AB-dCMP or AB-dUMP (~10-Å tether), seven on the transcribed strand (A) and seven on the nontranscribed strand (B) at the nucleotide positions indicated, were used in photoaffinity labeling experiments. The odd-numbered lanes contained B″, BRF, TBP, and TFIIIC, whereas the even-numbered lanes contained BRF, TBP, and TFIIIC only. The cross-linking efficiency of TBP at bp −23 (A, lanes 5 and 6) was seven- to ninefold higher with the addition of B″. Molecular weight markers are as described in the legend to Fig. 2.

and to ascertain the potential orientation of TBP in the complex, it was important to determine which region of TBP is cross-linked to the major groove of DNA at bp −23 in the transcribed strand. Identification of the region of TBP cross-linked to DNA at bp −23 was done by comparing the predicted cleavage products with the photoaffinity-labeled fragments of TBP from single-hit proteolysis. This approach has been successfully applied to the mapping of photoaffinity labeling sites of prokaryotic and eukaryotic RNA polymerases (5, 17, 37, 50, 52). Yeast TBP contains two cysteines at amino acids 78 and 164 and three internal methionines at amino acids 104, 121, and 197 (Fig. 7A).

Cleavage at cysteine residues was done with NTCB. NTCB modifies sulfhydryl groups in a protein, rendering them susceptible to alkaline hydrolysis (23). Single-hit cleavage with NTCB could potentially generate four fragments, two of which would have molecular masses of ~18 kDa and the other two of which would have molecular masses of ~8.5 kDa. An ~18-kDa labeled fragment would be expected if TBP were photoaffinity labeled between amino acids 79 and 164; an ~8.5-kDa fragment would be expected if either the N-terminal or the C-terminal region were photoaffinity labeled (amino acids 1 to 78 or 165 to 240, respectively). Photoaffinity-labeled TBP was partially cleaved with NTCB, and the predominant proteolytic

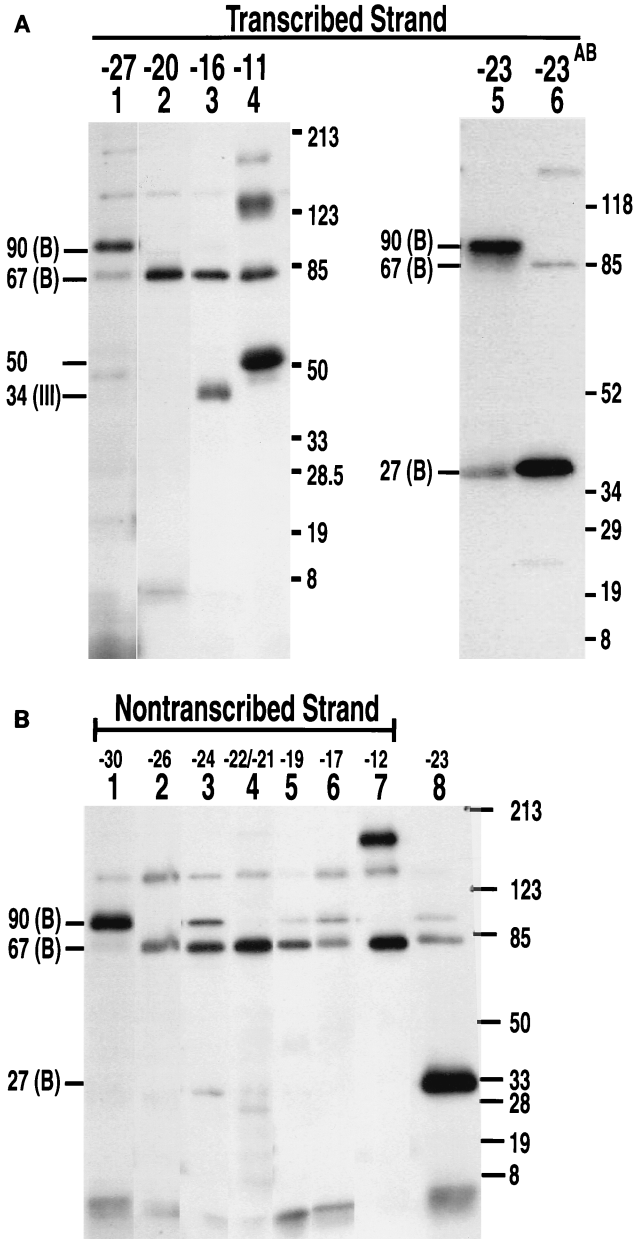

FIG. 5. Photocross-linking with DB probes revealed additional B″-DNA contacts at bp −27 and −23 on the transcribed strand and at bp −30 on the nontranscribed strand. Preinitiation complexes were formed as described in the legend to Fig. 3 with DNA probes containing DB-dUMP or DB-dCMP on the transcribed (A) and nontranscribed (B) strands and photocross-linked as described in the text. In lanes 6 in panel A and 8 in panel B, samples were photocross-linked with DNA probes containing AB-dCMP at bp −23 for comparison. Molecular weight markers are as described in the legend to Fig. 2.

product obtained (>90%) had a molecular mass of ~18 kDa. This result indicates that TBP was cross-linked in the region from amino acids 79 to 164 (Fig. 7B, lane 3). This region of TBP encompasses helices H1 and H2, β sheets S2 to S5, and most of β sheet S1′.

In order to further delineate the region of TBP that interacts with the major groove of DNA, cleavage at methionine residues was done with cyanogen bromide (Fig. 7A and C). A control sample and a molecular weight standard were created by engineering the cyclic AMP-dependent kinase site, GRRLSL, into wild-type TBP by changing cysteine 78 to arginine and aspartate 81 to serine. The mutant TBP was radiolabeled at serine 81 with [γ-^{35}S]adenosine-γ-thiotriphosphate and heart muscle kinase under conditions where wild-type TBP was not detectably phosphorylated (data not shown). The proteolytic fragments of ^{35}S-labeled TBP cleaved by cyanogen bromide and separated on a Tricine-SDS-polyacrylamide gel had relative molecular masses consistent with the expected phosphorylation site. These labeled proteolytic fragments of TBP were used as a molecular weight standard for the proteolytic fragments of photoaffinity-labeled TBP (Fig. 7C, lane 2). The presence of all three proteolytic cleavage products in approximately equal amounts indicates that all three internal methionine residues were equally cut by cyanogen bromide. The electrophoretic mobility of the phosphorylated TBP proteolytic fragments is expected to be slightly faster than that of fragments from photoaffinity-labeled TBP. Cleavage of the photoaffinity-labeled protein with formic acid and diphenylamine cleaves DNA at purine residues and leaves two phosphate groups attached to the cross-linked deoxycytidine (42), whereas the phosphorylated TBP proteolytic fragments have a single phosphate group coupled to serine.

The conditions for chemical cleavage of the DNA cross-linked to TBP results in cutting at the Asp-Pro located at amino acids 19 and 20 (Fig. 7A). Chemical cleavage of the DNA with diphenylamine and formic acid resulted in ~17% of the protein being cleaved at the Asp-Pro site and generated a labeled 24.3-kDa fragment of TBP (Fig. 7C, lane 3). Cyanogen bromide cleavage of TBP under these conditions creates two sets of fragments: the primary products from the cyanogen bromide cleavage only and a set of less abundant fragments that are the result of cleavage at Asp-Pro and at a single methionine (Fig. 7A). Photoaffinity-labeled TBP cleaved with cyanogen bromide for 10 min produced three fragments having molecular masses of approximately 21.9, 13.4, and 11.5 kDa (Fig. 7C, lane 4). The lack of labeled proteolytic fragments of ~2.9 kDa (amino acids 1 to 19) and ~4.9 kDa (amino acids 198 to 240) shows that TBP is not cross-linked at the N or C terminus and is consistent with the NTCB cleavage results. The clear identification of the 13.4-kDa fragment was not possible, since it could correspond to proteolytic fragments from amino acids 1 to 121 or 122 to 140. The small amount of labeled 11.5-kDa fragment could be due to less efficient labeling at sites between amino acids 1 and 104 or to fivefold less efficient cutting at the Asp-Pro site, resulting in an 11-kDa fragment (amino acids 21 to 121). A 15.3-kDa labeled fragment could be expected and may be evident migrating slightly more slowly than the 13.4-kDa fragment. The ambiguities mentioned made it necessary to do extensive cyanogen bromide cleavage to better define the cross-linking site on TBP. Three fragments with molecular masses of 11.5 kDa (amino acids 1 to 104), 8.5 kDa (amino acids 122 to 197), and 1.9 kDa (amino acids 104 to 120) could be expected. The primary product obtained was an ~2-kDa fragment that unequivocally corresponds to the region of TBP between amino acids 105 and 120 (Fig. 7C, lane 5). The region of TBP from amino acids 105 to 120 corresponds to β sheet S4 and to edges of the S3 and S5 β sheets that are part of the surface of TBP shown to contact the minor groove of the TATA element (33).

The region encompassing β sheet S4 of TBP is thus shown to be in close contact with the major groove of DNA at bp −23 on the transcribed strand as part of the fully assembled TFIIIB-DNA complex. It is evident that at this position in the TFIIIB-DNA complex, the TBP-DNA contacts deviate from those in the TBP-TATA DNA complex. The photoreactive group at bp −23 would be too far from TBP and sterically hindered to

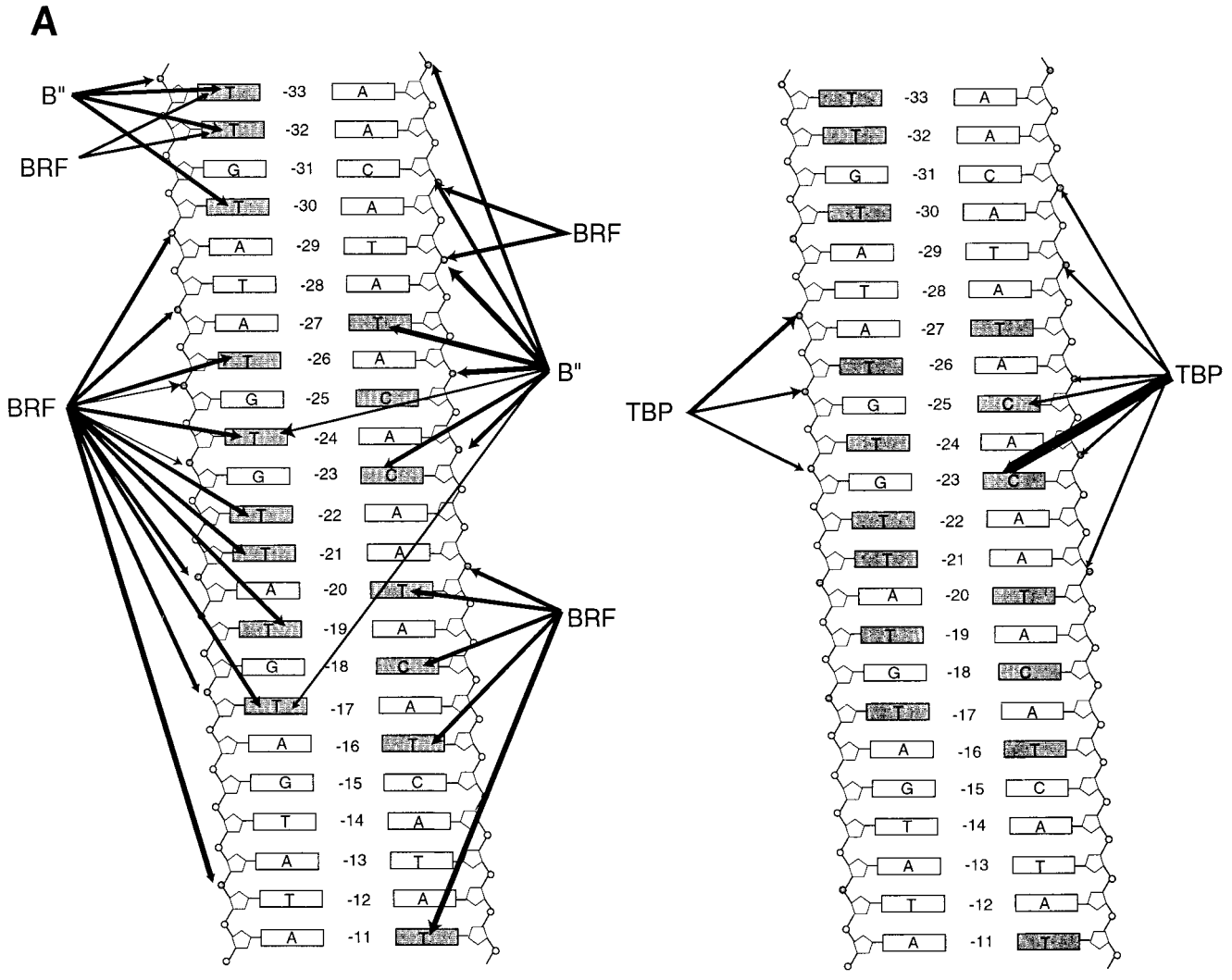

FIG. 6. BRF and B″ bind to opposite sides of the TBP-DNA complex. (A) Summary of DNA cross-linking to the BRF, B″, and TBP subunits of TFIIIB within the region upstream of the start site of the *SUP4* tRNA gene. The thickness of the arrows indicates the relative efficiency of cross-linking at each position. Bases and phosphodiester bonds that were modified are shaded. The BRF and B″ cross-links are displayed on the left, and those of TBP are displayed on the right. (B to D) The space-filling model of the TBP-TATA element complex is shown with TBP in magenta and DNA in gray (33). DNA positions that have been shown to be photocross-linked to BRF and B″ are highlighted in green and blue, respectively. The DNA structure has been modified from the original in that B-DNA has been added to both ends of DNA and the original DNA hairpin has been removed with the molecular modeling program Midas. One side of TBP is shown in panel B, and the structure is rotated 180° in panel C to visualize the other side of TBP. TBP is shown in ribbon form in panel D to better visualize the upstream or N-terminal stirrup region of TBP, and the structure is oriented such that the stirrup of TBP can be seen interacting with the minor groove of DNA. Illustrations were generated with RasMol version 2.6. TS, transcribed strand; NTS, nontranscribed strand.

cross-link TBP if it were in the same conformation as in the TBP-TATA DNA complex (Fig. 8). Although the exact amino acid cross-linked to DNA at bp −23 has not been determined, it can be inferred because of the strong preference of dehydroazepine (generated from phenylnitrene) for nucleophilic side chains. In the region from amino acids 105 to 120 (Fig. 8, yellow), several nucleophilic amino acids are located on both sides of TBP (nucleophilic groups in black). The region of TBP bound close to the minor groove in the TBP-TATA DNA complex is devoid of exposed nucleophilic side chains. TBP is most likely cross-linked to bp −23 at lysine 120 and/or serine 118, because of steric constraints and the close proximity of these sites to bp −23. If DNA at bp −23 contacted the other side of TBP (Arg 105, Thr 112, or Lys 110), then the DNA (i) would be entering and exiting near the same surface of TBP and (ii) would require a larger deviation from the TBP-TATA DNA structure (Fig. 8).

DISCUSSION

The topography of the core region of the TFIIIB-DNA complex was investigated by focusing on a 10- to 15-bp region of DNA centered ~25 bp upstream of the start site of transcription and containing a TATA-like sequence. In this complex, TFIIIB was recruited to DNA through protein-protein interactions with TFIIIC bound to the downstream promoter elements box A and box B. The interactions of all three subunits of TFIIIB (TBP, BRF, and B″) with the major and minor grooves of DNA were mapped by DNA photoaffinity labeling. DNA was modified by tethering a photoreactive group either

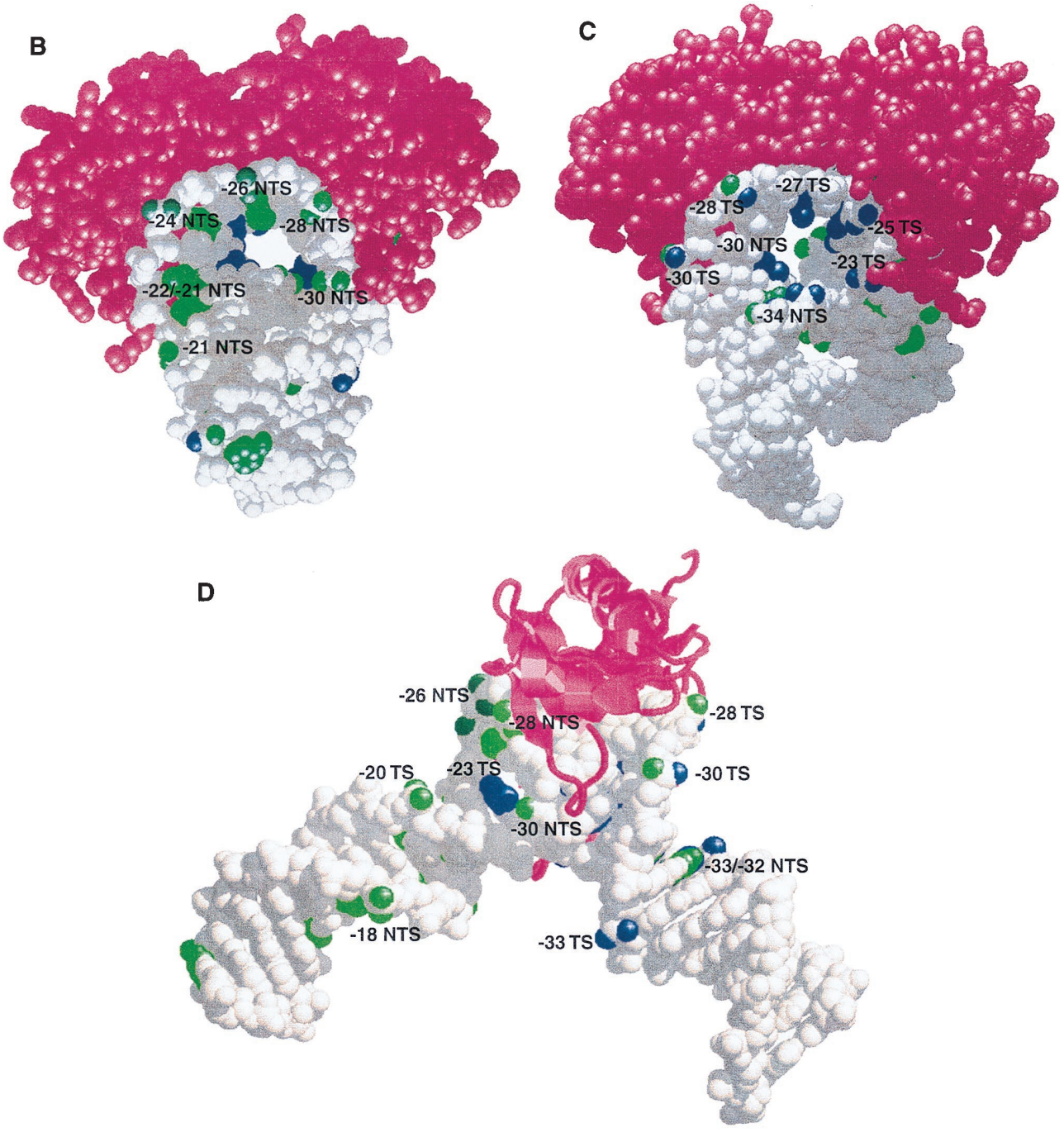

FIG. 6—*Continued.*

from the phosphate backbone into the major and minor grooves (SP probes) or from the nucleotide base into only the major groove (AB or DB probes). Cross-linking results obtained with the AB and DB probes revealed which proteins interact with the major groove near specific sites; with SP probes, proteins interacting with the minor groove were also determined. In this manner, it was shown that TBP is in close contact with the TATA-like sequence TATATGTG, which starts 30 nucleotides upstream of the start site of transcription of the *SUP4* $tRNA^{Tyr}$ gene. TBP contacts within this segment of DNA are primarily with the minor groove of DNA, as evidenced by cross-linking of TBP by the S-P probes and not by the AB probes at most positions tested in this region. These cross-linking data demonstrate that the interactions of TBP with DNA in a TFIIIB-DNA complex are similar to those of TBP bound to a TATA box, where it primarily contacts the minor groove of DNA.

Other evidence for TBP binding to DNA in the TFIIIB-DNA complex in a manner similar to that with the Pol II TATA box has been shown by Joazeiro and colleagues (24). Although TFIIIC recruits and promotes the binding of TFIIIB to DNA upstream of the start site of transcription, it was

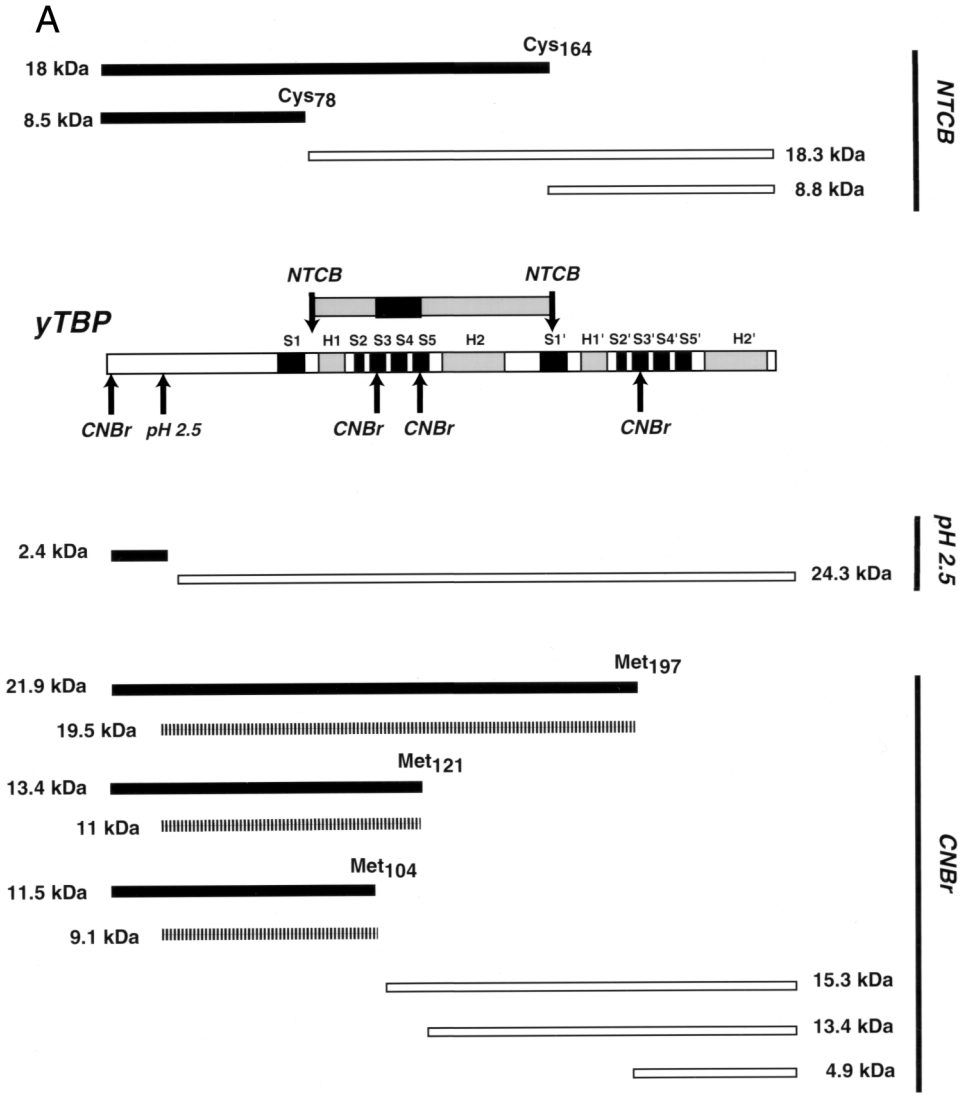
A
18 kDa
Cys164
8.5 kDa
Cys78
18.3 kDa
8.8 kDa
NTCB
yTBP
NTCB
NTCB
S1 H1 S2 S3 S4 S5 H2 S1' H1' S2' S3' S4' S5' H2'
CNBr
pH 2.5
CNBr
CNBr
CNBr
2.4 kDa
24.3 kDa
pH 2.5
21.9 kDa
Met197
19.5 kDa
13.4 kDa
Met121
11 kDa
11.5 kDa
Met104
9.1 kDa
15.3 kDa
13.4 kDa
4.9 kDa
CNBr

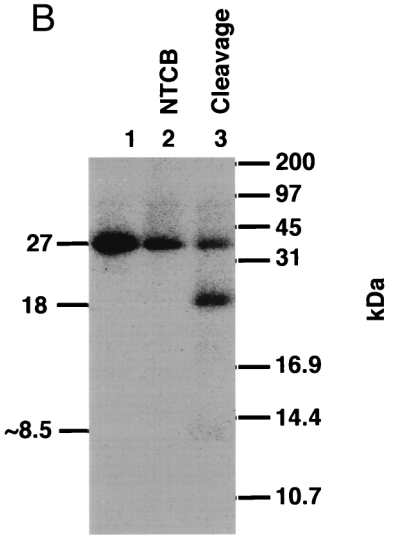
B
NTCB
Cleavage
1 2 3
200
97
45
31
27
18
16.9
~8.5
14.4
10.7

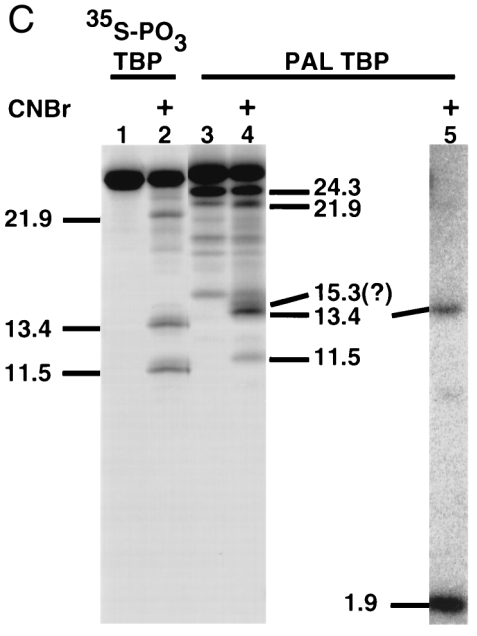
C
35S-PO3
TBP
PAL TBP
CNBr
+ + +
1 2 3 4 5
kDa
21.9
13.4
11.5
24.3
21.9
15.3(?)
13.4
11.5
1.9

shown that TATA sequences in this region influence the binding of TFIIIB within a certain distance from *box A*. The transcriptional start site and DNase I footprint of TFIIIB were altered by shifting the position of a TATA sequence within the TFIIIB binding region. TFIIIB reconstituted with an altered-specificity mutant of TBP (TBPm3) was properly positioned by use of the mutant TATA sequence TGTAAA, whereas wild-type TFIIIB was unable to bind to this sequence. These data indicate that (i) TBP does bind to DNA in the TFIIIB-DNA complex to help influence its position on DNA and (ii) its DNA binding characteristics are similar to those of TBP alone binding to the TATA element.

Given the evidence of the similarity of the DNA binding properties of TBP alone to those of TFIIIB, our DNA photocross-linking data were correlated to the known crystal structure of TBP bound to the TATA element. This analysis revealed that BRF and B″ form a protein clamp on the TBP-DNA complex with BRF binding to one side of the TBP-DNA complex and B″ binding to the opposite side. The major groove of the ~8-bp TATA sequence is pushed in toward itself to create a highly condensed region of DNA that serves as a scaffold for the interactions of BRF and B″. Mapping of the DNA contact sites of BRF indicates that BRF binds to the outer layer of one side of this core region. Additional BRF contacts are found to encompass the C-terminal stirrup of TBP, the same stirrup region that interacts with the core region of TFIIB, as shown in the TFIIB-TBP-TATA crystal structure (40).

The region surrounding the N-terminal stirrup of TBP had been shown in two separate studies to be important for BRF binding (11, 45). One approach was to make radical amino acid changes on the surface of TBP by site-directed mutagenesis to determine which residues of TBP are critical for the binding of BRF. A second approach was to show that TFIIA competes for the binding of BRF to the TBP-DNA complex, whereas TFIIB does not compete for binding (11). The crystal structure of TFIIA-TBP-DNA has shown that TFIIA interacts with the N-terminal stirrup of TBP, the stirrup opposite that contacted by TFIIB (48). At first glance, these data and the results discussed earlier indicating that BRF is bound close to the C-terminal stirrup may appear to be conflicting. First, it is important to note that the interactions being examined in these studies are those of TBP alone bound to a TATA box with BRF. The N-terminal stirrup of TBP is therefore important for the preliminary contact between BRF and TBP, but additional interactions between BRF and TBP are likely to exist in the TFIIIB-DNA complex. We and others have obtained cross-linking data showing that the region of BRF showing sequence homology to TFIIB is cross-linked to DNA near the 5′ end of the TATA-like region (reference 29 and results not shown). The BRF contacts with DNA between bp −26 and −30 are dependent on the presence of B″ and suggest that the interactions of BRF with the C-terminal stirrup of TBP are B″ dependent. B″ makes extensive contacts within the core region of the major groove of DNA as it extends into this area from the side of the TBP-DNA complex opposite that bound by BRF. A TBP mutant (E93R) that has been shown to be defective only in the binding of B″ is located on the same side of TBP as that shown to make contact with B″ by DNA photocross-linking (11). The surface of B″ making contact with the core region of DNA appears to be fairly devoid of nucleophilic side chains, probably entails a more hydrophobic region of the protein, as evidenced by cross-linking preference, and may help account for the nonionic binding properties of TFIIIB. At bp −23 in the transcribed strand, B″ was cross-linked with phenyldiazirine-containing probes (DB probes) and not with phenylazide-containing probes (AB probes). Although not as pronounced, the same cross-linking preference was also observed at bp −27 (transcribed strand) and bp −30 (nontranscribed strand) for B″. Aryl azides have a strong preference for nucleophilic side chains, whereas phenyldiazirines are more reactive, with no obvious side-chain preference (4, 8, 49). The protein clamp formed by sandwiching TBP on one side with BRF and on the other side with B″ is likely to be responsible for the stability of the TFIIIB-DNA complex in the presence of high salt and polyanions.

Most of the DNA photocross-linking data are consistent with the canonical TBP-TATA element crystal structure, except for the very strong cross-linking of TBP in the major groove at bp −23. The highly efficient cross-linking of TBP with AB-dCMP and not with DB-dCMP at bp −23 indicates that a nucleophilic surface of TBP is in close contact with the major groove of DNA at this position. Peptide mapping of TBP photoaffinity labeled at bp −23 revealed that the region of TBP from amino acids 105 to 120 is close to the major groove of DNA at bp −23. The implications of this data are twofold. First, the demonstration of this region of TBP contacting the 3′ side of the TATA-like sequence shows that TBP is oriented in the same direction on a tRNA gene as on a TATA-containing gene transcribed by Pol II. The orientation of TBP on the DNA is important to determine, because TBP appears not to have a strong orientation specificity, as the TBP homolog of *Pyrococcus woesei* has an orientation opposite that of the TBP-TATA box structure in eukaryotes (12, 34, 51). Second, the trajectory of DNA as it exits the downstream half of the TBP-DNA complex must be different from that in the TBP-TATA box complex. The distance from bp −23 to the cross-linked region of TBP is too large (≥15 Å) and there is too much steric interference for this cross-linking to occur if the structure of the core DNA with TBP were the same as the TBP-TATA box crystal structure.

We can postulate two models that would be consistent with the TBP-DNA cross-linking data at bp −23 and that differ by which side of TBP the DNA contacts as it exits from the 3′ end of the complex. The region of TBP from amino acids 105 to 120 includes nucleophilic amino acids that are found on both sides of TBP, as shown in Fig. 8, and are the putative cross-

FIG. 7. The region of TBP centered around β sheet S4 is cross-linked to the major groove of DNA at bp −23 in the TFIIIB-DNA complex. (A) Yeast TBP (yTBP) is schematically depicted with alpha helices marked by bars labeled H1, H1′, H2, and H2′ and beta sheets depicted by bars labeled S1 to S5 and S1′ to S5′ (33). CNBr and NTCB cleave at methionine and cysteine residues, respectively, and formic acid (pH 2.5) cleaves at Asp-Pro linkages. The several cleavage sites are indicated above and below TBP by arrows. Proteolytic fragments that would be expected from a single-hit digestion with each of these reagents are shown with their predicted molecular masses. Secondary and less abundant proteolytic fragments that could be obtained by a combination of formic acid cleavage and cyanogen bromide cleavage are indicated by hatched bars. The region of TBP cross-linked to DNA is shown above the TBP sequence; the primary cross-linking site is represented by the box in the center, with flanking regions on each side. (B) Gel-purified, photoaffinity-labeled TBP (lane 1) was modified with NTCB (lane 2) and then cleaved by alkaline hydrolysis (lane 3) to generate predominantly an 18-kDa fragment. (C) Mutant TBP (lanes 1 to 3) with a cyclic AMP-dependent kinase site engineered at amino acid 78 was phosphorylated with heart muscle kinase and [γ-^{35}S]adenosine-γ-thiotriphosphate. Phosphorylated TBP and photoaffinity-labeled (PAL) TBP were gel purified and cleaved with cyanogen bromide for 10 min (lanes 2 and 4). The cleavage products were analyzed by Tricine-SDS-polyacrylamide gel electrophoresis and subsequent autoradiography. Lane 5 contained photoaffinity-labeled TBP that was exhaustively digested with cyanogen bromide after being electroblotted onto a PVDF membrane. The molecular masses (in kilodaltons) of the fragments are indicated to the left and right of the lanes.

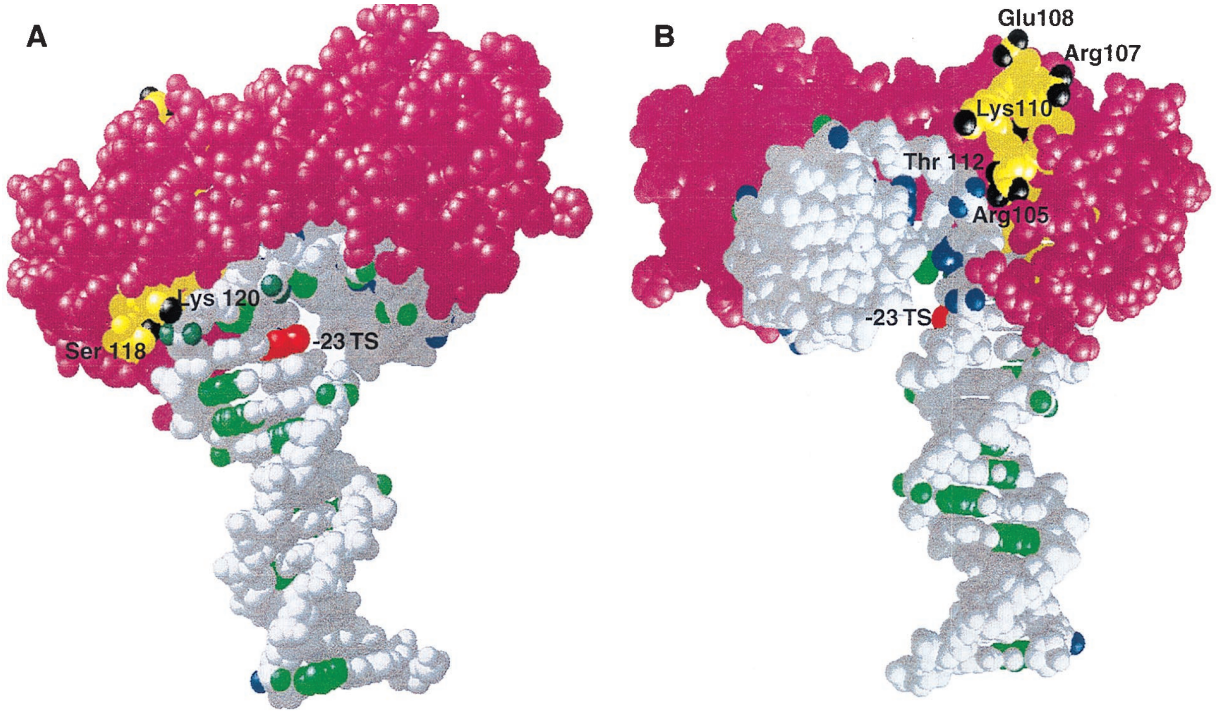

FIG. 8. The interaction of TBP with the 3′ half of the TATA-like sequence in the TFIIIB-DNA complex is not the same as that of the TBP-TATA box complex. The region of DNA at bp −23 on the transcribed strand (TS) that cross-links TBP is highlighted in red by use of the same model as that shown in Fig. 6. The region of TBP cross-linked to bp −23 is highlighted in yellow, and the nucleophilic groups present in this region are shown in black. (A) The TBP-TATA box structure is shown to reveal one side of TBP with DNA projecting down from TBP and toward the transcription start site. The nucleophilic groups on this side of TBP that are within the region cross-linked to DNA are labeled (Lys 120 and Ser 118). (B) The TBP-TATA box structure is shown to reveal the opposite side of TBP (relative to that in panel A) with the upstream portion of DNA pointing directly outward. The nucleophilic side chains on this side of TBP are labeled as in panel A. DNA positions cross-linked to BRF and B″ are highlighted in green and blue, respectively, except at bp −23.

linking sites. Changes in the trajectory of the DNA could be due to changes in the kinking of DNA near bp −23. TBP bends the TATA element by kinking DNA at two positions near the ends of the complex by inserting pairs of phenylalanines into the minor groove (33). One of these two positions is located between bp 7 and 8 in the TATA element and corresponds to bp −24 and −23 in the TATA-like sequence of the *SUP4* tRNA gene. Elimination of the kink between bp −24 and −23 could help bring the major groove of DNA at bp −23 into closer proximity to Lys 120 and Ser 118 of TBP. This model would position the downstream DNA on the side of TBP that would be consistent with BRF binding to one side of TBP. Another model, with the B″ side of TBP contacting the major groove at bp −23, is less likely because of (i) the drastic change in the trajectory of DNA required to bring bp −23 close to Arg 105, Thr 112, and Lys 110 and (ii) the potential steric clash of the DNA entering and exiting TBP on the same side of TBP.

B″ was shown to have an important role in the formation of TBP contacts with the major groove of DNA at bp −23. TBP cross-linking at bp −23 is enhanced ninefold by the addition of B″, while at other positions, the cross-linking of TBP is eliminated. The reduction of TBP cross-linking at these positions could be caused by efficient competition for the photoreactive group by BRF and B″ bound at these regions or by more site-selective placement of TBP in the presence of B″. Another indication that B″ is involved in changing DNA contacts at bp −23 is the observation that B″ also makes close contact with DNA at this position. B″ is efficiently cross-linked by the S-P probes at bp −25 and −23 and, when the phenylazide is replaced with a phenyldiazirine, B″ is the most efficiently cross-linked protein at bp −23 (transcribed strand). B″ is less efficiently cross-linked at bp −24 (nontranscribed strand) with DB-dUMP, consistent with B″ binding to DNA at this site.

Our evidence for the change in DNA trajectory in the TFIIIB complex from that of TBP bound to a TATA box is consistent with the DNA bending data for TFIIIB (6, 36). TFIIIB bound either to a tRNA gene or to the 5S rRNA gene bent DNA to a larger degree than TBP bound to the TATA box (46). After adjustment for the intrinsic bend in the *SUP4* tRNA gene, the bend angle for TFIIIB was ~115 to 135°; with the 5S rRNA gene, it was ~105 to 140°. In comparison, the bend angle for TBP on the adenovirus major late promoter was ~95°. The observation for the 5S rRNA gene that the TFIIIB-DNA complex devoid of B″ was not as bent as the complete TFIIIB-DNA complex coincides with our results indicating that the altered path of the 3′ half of the TATA element DNA on TBP required the B″ subunit.

DNA photoaffinity labeling continues to provide more details on the topography of Pol III transcription as different kinds of photoreagents are used and the data are correlated to the known X-ray crystallographic structures of some of the components of the transcription complex. Together, topological mapping by site-specific cross-linking and X-ray crystallographic analysis of subcomponents of the complex make it possible to obtain a comprehensive view of large protein assemblies such as that of the eukaryotic transcription complex. This study has also shown the need to use several different kinds of photoreagents to obtain complementary information. Finally, the kind of information obtained from DNA cross-linking is substantially enhanced when the region of the pro-

tein cross-linked is identified to better define the protein region interacting with DNA.

ACKNOWLEDGMENTS

We thank Tony Weil for anti-TBP antibody and Steve Edmondson for assistance in modeling the TBP-DNA complex.

This work was supported by Public Health Service grant GM 48413 from the National Institute of General Medical Sciences.

Jim Persinger and Sarojini M. Sengupta contributed equally to this work.

REFERENCES

1. **Bartholomew, B., D. Durkovich, G. A. Kassavetis, and E. P. Geiduschek.** 1993. Orientation and topography of RNA polymerase III in transcription complexes. Mol. Cell. Biol. **13:**942–952.
2. **Bartholomew, B., G. A. Kassavetis, B. R. Braun, and E. P. Geiduschek.** 1990. The subunit structure of Saccharomyces cerevisiae transcription factor IIIC probed with a novel photocrosslinking reagent. EMBO J. **9:**2197–2205.
3. **Bartholomew, B., G. A. Kassavetis, and E. P. Geiduschek.** 1991. Two components of Saccharomyces cerevisiae transcription factor IIIB (TFIIIB) are stereospecifically located upstream of a tRNA gene and interact with the second-largest subunit of TFIIIC. Mol. Cell. Biol. **11:**5181–5189.
4. **Bayley, H.** 1983. Photogenerated reagents in biochemistry and molecular biology, vol. 12. Elsevier Biomedical Press, Amsterdam.
5. **Borukhov, S., J. Lee, and A. Goldfarb.** 1991. Mapping of a contact for the RNA 3′ terminus in the largest subunit of RNA polymerase. J. Biol. Chem. **266:**23932–23935.
6. **Braun, B. R., G. A. Kassavetis, and E. P. Geiduschek.** 1992. Bending of the Saccharomyces cerevisiae 5S rRNA gene in transcription factor complexes. J. Biol. Chem. **267:**22562–22569.
7. **Brow, D. A., and C. Guthrie.** 1990. Transcription of a yeast U6 snRNA gene requires a polymerase III promoter element in a novel position. Genes Dev. **4:**1345–1356.
8. **Brunner, J.** 1993. New photolabeling and crosslinking methods. Annu. Rev. Biochem. **62:**483–514.
9. **Burnol, A. F., F. Margottin, J. Huet, G. Almouzni, M. N. Prioleau, M. Mechali, and A. Sentenac.** 1993. TFIIIC relieves repression of U6 snRNA transcription by chromatin. Nature **362:**475–477.
10. **Colbert, T., and S. Hahn.** 1992. A yeast TFIIB-related factor involved in RNA polymerase III transcription. Genes Dev. **6:**1940–1949.
11. **Colbert, T., S. Lee, G. Schimmack, and S. Hahn.** 1998. Architecture of protein and DNA contacts within the TFIIIB-DNA complex. Mol. Cell. Biol. **18:**1682–1691.
12. **Cox, J. M., M. M. Hayward, J. F. Sanchez, L. D. Gegnas, S. van der Zee, J. H. Dennis, P. B. Sigler, and A. Schepartz.** 1997. Bidirectional binding of the TATA box binding protein to the TATA box. Proc. Natl. Acad. Sci. USA **94:**13475–13480.
13. **Eschenlauer, J. B., M. W. Kaiser, V. L. Gerlach, and D. A. Brow.** 1993. Architecture of a yeast U6 RNA gene promoter. Mol. Cell. Biol. **13:**3015–3026.
14. **Fleming, S. A.** 1995. Chemical reagents in photoaffinity labeling. Tetrahedron **51:**12479–12520.
15. **Gerlach, V. L., S. K. Whitehall, E. P. Geiduschek, and D. A. Brow.** 1995. TFIIIB placement on a yeast U6 RNA gene in vivo is directed primarily by TFIIIC rather than by sequence-specific DNA contacts. Mol. Cell. Biol. **15:**1455–1466.
16. **Goodrich, J. A., and R. Tjian.** 1994. TBP-TAF complexes: selectivity factors for eukaryotic transcription. Curr. Opin. Cell. Biol. **6:**403–409.
17. **Grachev, M. A., E. A. Lukhtanov, A. A. Mustaev, E. Zaychikov, M. N. Abdukayama, I. V. Rabinov, V. I. Richter, Y. S. Skoblov, and P. G. Chistyakov.** 1989. Studies of the functional topography of *Escherichia coli* RNA polymerase. Eur. J. Biochem. **180:**577–585.
18. **Grove, A., A. Galeone, E. Yu, L. Mayol, and E. P. Geiduschek.** 1998. Affinity, stability, and polarity of binding of the TATA binding protein governed by flexure at the TATA box. J. Mol. Biol. **282:**731–739.
19. **Hernandez, N.** 1993. TBP, a universal eukaryotic transcription factor? Genes Dev. **7:**1291–1308.
20. **Hoopes, B. C., J. F. LeBlanc, and D. K. Hawley.** 1998. Contributions of the TATA box sequence to rate-limiting steps in transcription initiation by RNA polymerase II. J. Mol. Biol. **277:**1015–1031.
21. **Hoopes, B. C., J. F. LeBlanc, and D. K. Hawley.** 1992. Kinetic analysis of yeast TFIID-TATA box complex formation suggests a multi-step pathway. J. Biol. Chem. **267:**11539–11547.
22. **Horikoshi, M., T. Yamamoto, Y. Ohkuma, P. A. Weil, and R. G. Roeder.** 1990. Analysis of structure-function relationships of yeast TATA box binding factor TFIID. Cell **61:**1171–1178.
23. **Jacobson, G. R., M. H. Schaffer, G. R. Stark, and T. C. Vanaman.** 1973. Specific chemical cleavage in high yield at the amino peptide bonds of cysteine and cystine residues. J. Biol. Chem. **248:**6583–6591.
24. **Joazeiro, C. A., G. A. Kassavetis, and E. P. Geiduschek.** 1996. Alternative outcomes in assembly of promoter complexes: the roles of TBP and a flexible linker in placing TFIIIB on tRNA genes. Genes Dev. **10:**725–739.
25. **Kassavetis, G. A., C. Bardeleben, B. Bartholomew, B. R. Braun, C. A. P. Joazeiro, M. Pisano, and E. P. Geiduschek.** 1994. Transcription by RNA polymerase III, p. 107–126. *In* R. C. Conaway and J. W. Conaway (ed.), Transcription: mechanisms and regulation. Raven Press, Ltd., New York, N.Y.
26. **Kassavetis, G. A., B. Bartholomew, J. A. Blanco, T. E. Johnson, and E. P. Geiduschek.** 1991. Two essential components of the Saccharomyces cerevisiae transcription factor TFIIIB: transcription and DNA-binding properties. Proc. Natl. Acad. Sci. USA **88:**7308–7312.
27. **Kassavetis, G. A., B. R. Braun, L. H. Nguyen, and E. P. Geiduschek.** 1990. S. cerevisiae TFIIIB is the transcription initiation factor proper of RNA polymerase III, while TFIIIA and TFIIIC are assembly factors. Cell **60:**235–245.
28. **Kassavetis, G. A., C. A. Joazeiro, M. Pisano, E. P. Geiduschek, T. Colbert, S. Hahn, and J. A. Blanco.** 1992. The role of the TATA-binding protein in the assembly and function of the multisubunit yeast RNA polymerase III transcription factor, TFIIIB. Cell **71:**1055–1064.
29. **Kassavetis, G. A., A. Kumar, E. Ramirez, and E. P. Geiduschek.** 1998. Functional and structural organization of Brf, the TFIIB-related component of the RNA polymerase III transcription initiation complex. Mol. Cell. Biol. **18:**5587–5599.
30. **Kassavetis, G. A., S. T. Nguyen, R. Kobayashi, A. Kumar, E. P. Geiduschek, and M. Pisano.** 1995. Cloning, expression, and function of TFC5, the gene encoding the B″ component of the Saccharomyces cerevisiae RNA polymerase III transcription factor TFIIIB. Proc. Natl. Acad. Sci. USA **92:**9786–9790.
31. **Kassavetis, G. A., D. L. Riggs, R. Negri, L. H. Nguyen, and E. P. Geiduschek.** 1989. Transcription factor IIIB generates extended DNA interactions in RNA polymerase III transcription complexes on tRNA genes. Mol. Cell. Biol. **9:**2551–2566.
32. **Kim, J. L., D. B. Nikolov, and S. K. Burley.** 1993. Co-crystal structure of TBP recognizing the minor groove of a TATA element. Nature **365:**520–527.
33. **Kim, Y., J. H. Geiger, S. Hahn, and P. B. Sigler.** 1993. Crystal structure of a yeast TBP/TATA-box complex. Nature **365:**512–520.
34. **Kosa, P. F., G. Ghosh, B. S. DeDecker, and P. B. Sigler.** 1997. The 2.1-A crystal structure of an archaeal preinitiation complex: TATA-box-binding protein/transcription factor (II)B core/TATA-box. Proc. Natl. Acad. Sci. USA **94:**6042–6047.
35. **Lannutti, B. J., J. Persinger, and B. Bartholomew.** 1996. Probing the protein-DNA contacts of a yeast RNA polymerase III transcription complex in a crude extract: solid phase synthesis of DNA photoaffinity probes containing a novel photoreactive deoxycytidine analog. Biochemistry **35:**9821–9831.
36. **Leveillard, T., G. A. Kassavetis, and E. P. Geiduschek.** 1991. Saccharomyces cerevisiae transcription factors IIIB and IIIC bend the DNA of a tRNA(Gln) gene. J. Biol. Chem. **266:**5162–5168.
37. **Markovtsov, V., A. Mustaev, and A. Goldfarb.** 1996. Protein-RNA interactions in the active center of transcription elongation complex. Proc. Natl. Acad. Sci. USA **93:**3221–3226.
38. **Nassal, N.** 1983. 4-(1-Azi-2,2,2-trifluoroethyl)benzoic acid, a highly photolabile carbine generating label readily fixable to biochemical agents. Liebigs Ann. Chem. **1983:**1510–1523.
39. **Nikolov, D. B., H. Chen, E. D. Halay, A. Hoffman, R. G. Roeder, and S. K. Burley.** 1996. Crystal structure of a human TATA box-binding protein/TATA element complex. Proc. Natl. Acad. Sci. USA **93:**4862–4867.
40. **Nikolov, D. B., H. Chen, E. D. Halay, A. A. Usheva, K. Hisatake, D. K. Lee, R. G. Roeder, and S. K. Burley.** 1995. Crystal structure of a TFIIB-TBP-TATA-element ternary complex. Nature **377:**119–128.
41. **Persinger, J., and B. Bartholomew.** 1996. Mapping the contacts of yeast TFIIIB and RNA polymerase III at various distances from the major groove of DNA by DNA photoaffinity labeling. J. Biol. Chem. **271:**33039–33046.
42. **Pruss, D., B. Bartholomew, J. Persinger, J. Hayes, G. Arents, E. N. Moudrianakis, and A. P. Wolffe.** 1996. A new model for the nucleosome: linker histones bind inside the DNA gyres. Science **274:**614–617.
43. **Rigby, P. W.** 1993. Three in one and one in three: it all depends on TBP. Cell **72:**7–10.
44. **Schagger, H., and G. von Jagow.** 1987. Tricine-sodium dodecyl sulfate-polyacrylamide gel electrophoresis for the separation of proteins in the range from 1 to 100 kDa. Anal. Biochem. **166:**368–379.
45. **Shen, Y., G. A. Kassavetis, G. O. Bryant, and A. J. Berk.** 1998. Polymerase (Pol) III TATA box-binding protein (TBP)-associated factor Brf binds to a surface on TBP also required for activated Pol II transcription. Mol. Cell. Biol. **18:**1692–1700.
46. **Starr, D. B., B. C. Hoopes, and D. K. Hawley.** 1995. DNA bending is an important component of site-specific recognition by the TATA binding protein. J. Mol. Biol. **250:**434–446.
47. **Struhl, K.** 1994. Duality of TBP, the universal transcription factor. Science **263:**1103–1104.

48. **Tan, S., Y. Hunziker, D. F. Sargent, and T. J. Richmond.** 1996. Crystal structure of a yeast TFIIA/TBP/DNA complex. Nature **381:**127–151.
49. **Tate, J. J., J. Persinger, and B. Bartholomew.** 1998. Survey of four different photoreactive moieties for DNA photoaffinity labeling of yeast RNA polymerase III transcription complexes. Nucleic Acids Res. **26:** 1421–1426.
50. **Treich, I., C. Carles, A. Sentenac, and M. Riva.** 1992. Determination of lysine residues affinity labeled in the active site of yeast RNA polymerase II(B) by mutagenesis. Nucleic Acids Res. **20:**4721–4725.
51. **Whitehall, S. K., G. A. Kassavetis, and E. P. Geiduschek.** 1995. The symmetry of the yeast U6 RNA gene's TATA box and the orientation of the TATA-binding protein in yeast TFIIIB. Genes Dev. **9:**2974–2985.
52. **Zaychikov, E., E. Martin, L. Denissova, M. Kozlov, V. Markovtsov, M. Kashlev, H. Heumann, V. Nikiforov, A. Goldfarb, and A. Mustaev.** 1996. Mapping of catalytic residues in the RNA polymerase active center. Science **273:**107–109.